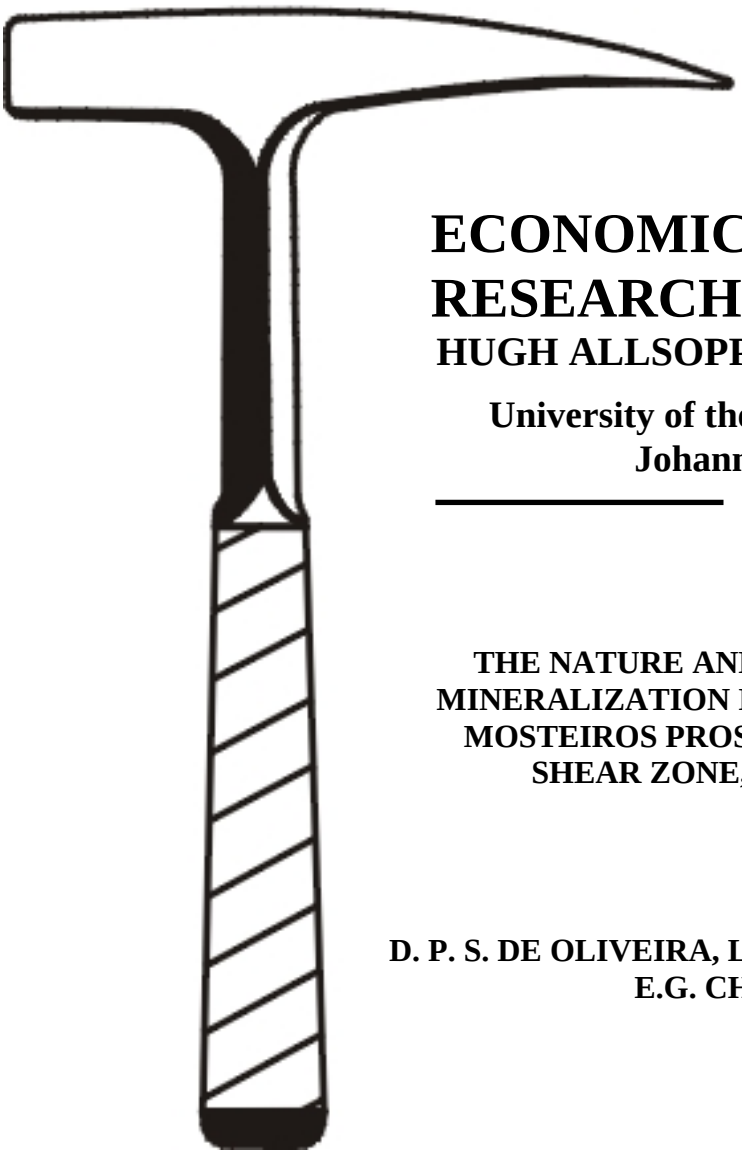

ECONOMIC GEOLOGY RESEARCH INSTITUTE

HUGH ALLSOPP LABORATORY

University of the Witwatersrand
Johannesburg

THE NATURE AND ORIGIN OF LODE-GOLD MINERALIZATION IN THE SÃO MARTINHO AND MOSTEIROS PROSPECTS, TOMAR CORDOBA SHEAR ZONE, EASTERN PORTUGAL

D. P. S. DE OLIVEIRA, L. J. ROBB, C. M.C. INVERNO and E.G. CHARLESWORTH

INFORMATION CIRCULAR No. 379

UNIVERSITYOF THE WITWATERSRAND
JOHANNESBURG

THE NATURE AND ORIGIN OF LODE-GOLD MINERALIZATION IN THE SÃO MARTINHO AND MOSTEIROS PROSPECTS, TOMAR CORDOBA SHEAR ZONE, EASTERN PORTUGAL

by

D. P. S. DE OLIVEIRA[1], L. J. ROBB[2], C. M.C. INVERNO[3] and E.G. CHARLESWORTH[4]

([1]Economic Geology Research Institute-Hugh Allsopp Laboratory, School of Geosciences,University of the Witwatersrand, Private Bag 3, WITS 2050, Johannesburg, South Africa;
Present address: Instituto Geológico e Mineiro, Apartado 7586, 2721-866 Alfragide, Portugal;
[2]Economic Geology Research Institute-Hugh Allsopp Laboratory (EGRI-HAL), School of Geosciences, University of the Witwatersrand, Private Bag 3, WITS 2050, Johannesburg, South Africa;
[3]Instituto Geológico e Mineiro, Apartado 7586, 2721-866 Alfragide (Lisbon), Portugal and CREMINER, Faculdade Ciências, Univ. Lisboa, Edifício C6, Campo Grande, 1749-016 Lisboa, Portugal;
[4] Department of Geology, School of Geosciences, University of the Witwatersrand, , Private Bag 3, WITS 2050, Johannesburg, South Africa)

ECONOMIC GEOLOGY RESEARCH INSTITUTE
INFORMATION CIRCULAR No. 379

June 2004

THE NATURE AND ORIGIN OF LODE-GOLD MINERALIZATION IN THE SÃO MARTINHO AND MOSTEIROS PROSPECTS, TOMAR CORDOBA SHEAR ZONE, EASTERN PORTUGAL

ABSTRACT

The São Martinho and Mosteiros orogenic lode-gold prospects are located in east central Portugal within the Tomar Cordoba Shear Zone (TCSZ). This important shear zone trends NW-SE separating two major tectonostratigraphic zones within the Iberian massif: The Central Iberian Zone to the north and the Ossa Morena Zone to the south. The TCSZ comprises a geologically complex and diverse zone of intense deformation and metamorphism contemporaneous with a large sinistral displacement of up to 300 km, active during the Variscan Orogeny. Within the shear zone the rocks are arranged in a flower structure with the oldest rocks within its core, the Blastomylonitic Belt. The TCSZ is intruded by both syntectonic (syn-Variscan) and late- to post-tectonic granitoids and its NE sector is marked with Westphalian-age wrench faults. The gold prospects are hosted in rocks of the Neoproterozoic age Série Negra, which north of the Blastomylonitic Belt at Mosteiros, are metamorphosed to greenschist facies, while south of the Blastomylonitic Belt at São Martinho, are metamorphosed to amphibolite facies.

São Martinho is characterized by the occurrence of two distinct episodes of gold mineralization. The first, RS I, typically lode-gold mineralization, is disseminated and veinlet-type mineralization and is closely associated with foliation-parallel quartz I veinlets. The ore minerals for RS I are: deformed/stretched arsenopyrite I + pyrite I + pyrite II + chalcopyrite I' (?) chalcopyrite I + gold I. The second episode of mineralization (RS II) is late and is associated with quartz II veins that cross-cut the foliation and hypersaline fluids of probable magmatic origin. The paragenesis is characterized by arsenopyrite II + pyrrhotite II + pyrite III + chalcopyrite II + loellingite + gold II. At São Martinho some of the alteration packages are subtle and difficult to recognize apart from marked silicification, and consist of chloritization, muscovitization/sericitization ± tourmalinization, albitization and carbonatization products.

Mineralization is envisaged to occur after peak metamorphic conditions in the early Carboniferous, contemporaneous with the Variscan Orogeny, with the contribution of ore-forming fluids from metamorphic devolatilization reactions occurring within the Série Negra metasediments and, probably, from fluids supplied by crystallizing syntectonic granitoids. At São Martinho the formation of wrench faults in the Upper Carboniferous, during late-stage movements of the shear zone, allowed these to be used as conduits for hypersaline magmatic fluids derived from large, late- to post-tectonic granitic magmas. These fluids remobilized early-formed orogenic lode gold and redeposited gold associated with high-temperature minerals such as loellingite.

The Mosteiros prospect is characterized by being hosted in heavily carbonatized and brecciated felsic metatuffs of the Série Negra that have suffered pervasive ferroan dolomite alteration and also muscovitization, silicification, fuchsitization and chloritization and contain disseminated sulphide mineralization. Ilmenite, pyrite, arsenopyrite, chalcopyrite, tetrahedrite, pyrrhotite, gold and jamesonite were identified in Mosteiros. Gold is typically scarce and very small when observed, and also occurs as microscopic gold ("invisible gold") within the lattices of large euhedral pyrite grains and smaller euhedral arsenopyrite grains. The RS I mineralizing event in São Martinho has a few vague, but limited, similarities to the Mosteiros mineralizing event.

_____oOo_____

THE NATURE AND ORIGIN OF LODE-GOLD MINERALIZATION IN THE SÃO MARTINHO AND MOSTEIROS PROSPECTS, TOMAR CORDOBA SHEAR ZONE, EASTERN PORTUGAL

CONTENTS

_____oOo_____

Published by the Economic Geology Research Institute
(incorporating the Hugh Allsopp Laboratory)
School of Geosciences
University of the Witwatersrand
1 Jan Smuts Avenue
Johannesburg
South Africa
http://www.wits.ac.za/geosciences/egri.htm

ISBN 1-86838-345-8

THE NATURE AND ORIGIN OF LODE-GOLD MINERALIZATION IN THE SÃO MARTINHO AND MOSTEIROS PROSPECTS, TOMAR CORDOBA SHEAR ZONE, EASTERN PORTUGAL

INTRODUCTION

The precious metal potential of the Tomar Cordoba Shear Zone (TCSZ), which trends NW-SE from Tomar in central Portugal to Cordoba in SW Spain, remains to be fully evaluated and continues to be a promising gold exploration target within the Iberian Peninsula. As a result of fluctuating market conditions, gold exploration has been carried out intermittently by private companies and the Portuguese Geological Survey (IGM) in this area since the late 1980s. Within the TCSZ the São Martinho and Mosteiros prospects have been investigated in the present study in terms of the mode of occurrence of gold mineralization as well as its associated ore minerals, alteration assemblages and limited S-isotope studies. Based on these data and structural, fluid inclusion and geochronological data, a general ore-genesis model is proposed and the results obtained in this study are broadly compared to other worldwide orogenic lode-gold deposits.

GEOLOGICAL, STRUCTURAL AND METAMORPHIC SETTING

Geological and structural setting

The TCSZ forms the major terrane boundary between two major tectonostratigraphic subdivisions of the Iberian Massif (Julivert *et al.*, 1972; Ribeiro *et al.*, 1979): the Central Iberian Zone in the north and the Ossa Morena Zone in the south (Figs. 1A and B). The TCSZ represents a geologically complex and diverse zone of intense deformation and metamorphism contemporaneous with a large sinistral displacement, which may be due to a large intracontinental sinistral fault active during the Variscan Orogeny (Berthé *et al.*, 1979) with sinistral displacements estimated up to 100 km (Burg *et al.*, 1981) to 300 km (Abalos and Eguíluz, 1992a, b). This displacement caused mylonitization and retrograde metamorphism (under greenschist to amphibolite facies) to all previous Cadomian structures and mineral assemblages (Quesada and Munhá, 1990). Pereira and Silva (2001) considered the Tomar Cordoba Shear Zone a major Eovariscan-Variscan sinistral transcurrent fault overprinting a Cadomian arc localised at a convergent margin of Gondwana, although this interpretation has always been regarded as controversial (Azor *et al.*, 1994). The Cadomian, Avalonian, or Pan-African Orogeny (Late Proterozoic to Early Palaeozoic) arises from the reactivation of continental thickening and amalgamation of microcontinents; the Armorica microcontinent (made up of the Bohemian, Armorican, Iberian and Sardinian massifs) at the western boundary of Gondwana and the Avalonia microcontinent (made up of the Brabant and Ardennes massifs, Wales, southern Ireland, Avalon Peninsula, northern Nova Scotia and New England). It is generally accepted that these microcontinents included fragments of island and volcanic arcs formed during a process of continental convergence at the margins of the main continental masses in the Late Palaeozoic (Eguíluz *et al.*, 2000).

The Portuguese sector of the TCSZ comprises a series of polymetamorphic structural-tectonic subdomains defined by Pereira (1995, 1999; Fig. 1B). These subdomains are, from north to south, Urra-Mosteiros-Ouguela Subdomain, Degolados-Campo Maior Subdomain, Arronches-Morenos-Caia Subdomain, Assumar Subdomain and the Alter do Chão-Elvas Subdomain (Fig. 1B). Each of these subdomains is a thrust fault-bounded package of rocks and the thrust faults are arranged in a flower-like structure more or less centred in a core of migmatitic gneisses termed the Blastomylonitic Belt (Fig. 1C). Other, more recent studies

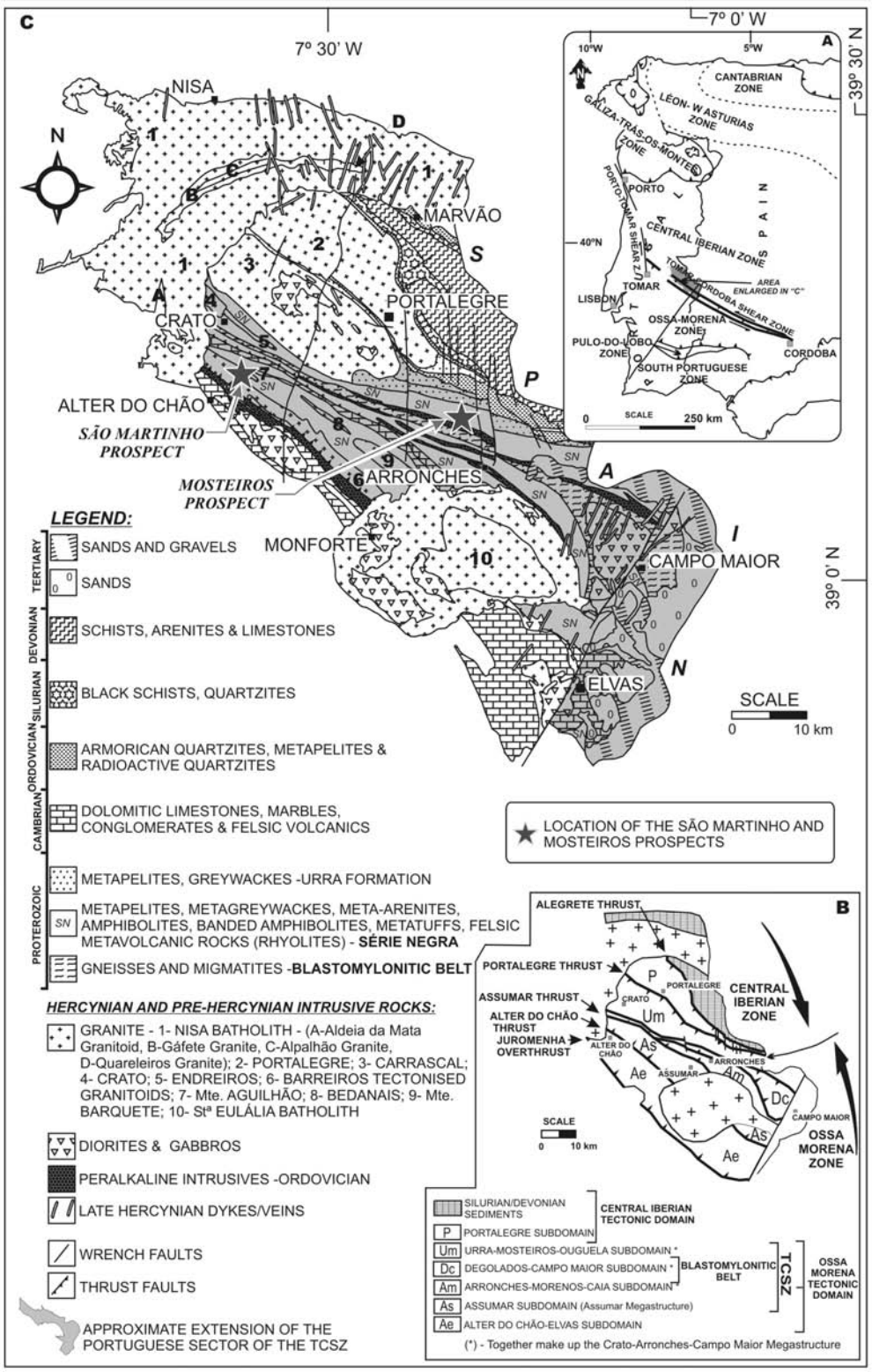

Figure 1: *A- Subdivision of the Hercynian Massif into tectonostratigraphic zones (after Quesada, 1992) and location of the study area; B- Subdivision of the TCSZ into the various subdomains (adapted after Pereira, 1995; 1999); C- Excerpt from the 1:500 000 geological map of Portugal (after Oliveira et al., 1992) showing the simplified geology of the TCSZ and surrounding areas as well as the location of the Mosteiros and São Martinho prospects. The various granite names with their various facies types are reproduced within each granitoid type. Nisa granite facies types are after Moreira (1994) and Solá (1996-1999).*

indicate that the complex geometry of this region reflects the structure developed during Variscan transcurrent movements parallel to the orogen trend and the TCSZ is made up of a system of composite flower-like structures with opposite NE- and SW-verging, narrow, asymmetric folds with steep axial planes, superimposed on previous Variscan and Cadomian tectonic fabrics (Pereira and Silva, 2002).

Within the TCSZ are exposed the Neoproterozoic (Schäfer *et al.*, 1993) Série Negra (*black series*) rocks - the name given as a result of the overwhelming majority of dark-coloured rocks that make up this series. The Série Negra crops out scarcely both north and south of the Blastomylonitic Belt. Stratigraphically, the Série Negra is made up of the (lower) Morenos and (upper) Mosteiros Formations.

The Morenos Formation is made up of micaceous schists, which are locally garnet-bearing, metalimestones and calc-silicate assemblages, meta-arkoses, meta-arenites (quartzites) and micaceous and siliceous schists, amphibolites and metapyroclastic rocks (Oliveira *et al.*, 1991). The Mosteiros Formation consists of black schists/slates, metagreywackes, black quartzites (De Oliveira *et al.*, 2003a; b), metalimestones and amphibolites (Oliveira *et al.*, 1991). North of the Blastomylonitic Belt, the Urra Formation unconformably overlies the Mosteiros Formation and is made up of a lower porphyry unit and an upper pale green pelite/greywacke unit (Oliveira *et al.*, 1991; De Oliveira, 1998). At the TCSZ borders, a (Lower) Cambrian sequence of platform sedimentary rocks is preserved, which unconformably overlies the Neoproterozoic Série Negra metasedimentary rocks (see Fig. 1C) and consists of micaceous schists, amphibolites, metamorphosed carbonate rocks and pelitic schists (Oliveira *et al.*, 1991).

The TCSZ is intruded by several pre-Variscan and late- to post-Variscan granitoids. The migmatitic gneisses within the Blastomylonitic Belt have, because of the flower-like structure arrangement of the rocks, always been considered to be the oldest rocks (Gonçalves and Carvalhosa, 1994). These migmatites have been dated at *c.* 1700 Ma ($^{207}Pb/^{206}Pb$ ages) by Ordoñes-Casado (1998). However, recent geochronology work by De Oliveira *et al.* (2002a) indicates that the protolith ages are much older with U-Pb ages of 2146 ± 91 Ma.

Within the TCSZ outcrop three elongated bodies of granite that have yet to be dated (the syntectonic Mte. Aguilhão, Bedanais and Mte. Barquete granites; Fig. 1C). Their elongate shape indicates ductile deformation during the Variscan Orogeny, which refers to an orogenic episode between Late Devonian and late Carboniferous (Eguíluz *et al.*, 2000).
The deformed Barreiros tectonized granitoids crop out at the southern border of the TCSZ. These granitoids yield weighted mean $^{207}Pb/^{206}Pb$ ages of 508 ± 8.1 Ma (De Oliveira *et al.*, 2002a).

The TCSZ is truncated in the NW and SE by two large granitic batholiths, the Nisa and Stª Eulália batholiths respectively (Fig. 1C) that are considered to be late- to post-Variscan in age. The Stª Eulália batholith is composed of four approximately concentric rings of different granitic compositions surrounding a central granodioritic to monzogranitic core (Carrilho Lopes *et al.*, 1997). The outer monzogranitic ring (the Referta granite) has been dated "at approximately 290 Ma" (errors and method not reported; Pinto *et al.*, 1987). These authors further pointed out that the central core is probably older at 306 Ma. However, Eguíluz *et al.* (2000) showed the Stª Eulália batholith to be 281 Ma old (Rb-Sr ages).

The Nisa batholith yields ages that vary between 309 and 287 Ma. Gonçalves and Fernandes (1973) stated that the Nisa batholith is Permian-Carboniferous in age (290 to 309 Ma), but

dating methods are not reported. In Pinto *et al.* (1987) the Nisa batholith is reported as being 306 Ma (Rb/Sr age) while Eguíluz *et al.* (2000) reported ages of 287 and 301 Ma using K-Ar. In addition, Menéndez (1998) showed two Rb-Sr isochrons with 289 ± 22 and 294 ± 11 Ma for two samples collected NNW of Albuquerque (Spanish side of the border, N of Badajoz).
Two phases of Variscan deformation were identified in the TCSZ (Gonçalves *et al.*, 1978). The first phase of deformation (D1) developed WSW-verging folds with NE-dipping axial planar schistosity (S1) with a tendency for the axial planes to become more horizontal as one moves southwestwards. The second phase of deformation (D2) generated folds with subvertical axial planes or axial planes strongly dipping to the NE and striking NW-SE. The D2 deformation generated refolding of the D1 structures and also developed a crenulation cleavage (S2) (Pereira, 1995).

The TCSZ is cut by N-S trending, quartz-filled, wrench faults/fractures of probable late Westphalian (314-305 Ma) age (Gonçalves *et al.*, 1978). They form a typical domino or bookshelf geometry (Roberts *et al.*, 1991; Gumiel and Campos, 2001) similar to that reported from areas of extensional and strike-slip tectonics. When these faults are traced eastwards of the Mosteiros prospect, they progressively rotate in an anticlockwise direction (Roberts *et al.*, 1991). These N-S faults are clearly visible in the northern sector of the TCSZ (Fig. 1C) and trenching carried out in the São Martinho prospect revealed rhyolite- and quartz-filled fault zones with a similar orientation (Camm, 1996).

Metamorphic setting of the Tomar Cordoba Shear Zone (TCSZ)

South of the Blastomylonitic Belt, the Série Negra shows amphibolite facies grade metamorphism evidenced by the large expanses of amphibolite and banded amphibolite outcrops (De Oliveira, 2001a; De Oliveira *et al.*, 2003c), while north of the Blastomylonitic Belt, the Série Negra shows greenschist facies grade metamorphism, which characteristically yields chloritic metapelitic sequences (Gonçalves, 1971). Metamorphic conditions for the gneisses in the Blastomylonitic Unit (Belt), in the Higuera de Llerena area in SW Spain, were established by Abalos *et al.* (1991a, b) using garnet core and rim composition and various geobarometers. Biotite-rich gneisses from the migmatitic (blastomylonitic) belt in this area experienced peak metamorphic conditions established at ~ 670 ± 30 ºC and 10.0 ± 0.5 kbar (average results from garnet cores) with an evolution towards lower P and T, ~ 610 ± 30 ºC and 6.7 ± 0.5 kbar as recorded by garnet rim compositions. Average age of partial melting, caused by migmatization, in the TCSZ is 335 ± 3 Ma (based on several samples from the previously mentioned Spanish locations), which is the age of new zircon domain formation in the leucosomes close to or at peak temperature (Ordoñes-Casado, 1998). Ordoñes-Casado's data are in agreement with a number of muscovite cooling ages published by Blatrix and Burg (1981) and Quesada and Dallmeyer (1994). Therefore, this age seems to record the peak temperature prior to rapid cooling after anatexis.

P-T conditions of eclogite facies metamorphism reached in excess of 15 kbar and 600-800 ºC (Abalos *et al.*, 1991b) and minimum conditions of 9-10 kbar and 750-800 ºC (Mata and Munhá, 1986a, b) were recorded on retrogressed eclogites in different parts of the TCSZ. Ages for retrogressed eclogites, using the SHRIMP technique, yield average (weighted mean) ages of 340 ± 13 Ma (Ordoñes Casado, 1998; p. 159) in zircon domains with low U and Th contents (ave. 51 and 2 ppm, respectively). Average Th/U ratios of 0.05, typical for metamorphic rocks, were obtained by Casado (1998). As these ages coincide with ages reported by Abalos *et al.* (1991b), the age of 340 ± 13 Ma is considered to be the age of high-pressure metamorphism (fig. 3.65 in Ordoñes-Casado, 1998).

The complete P-T path of metamorphism in the TCSZ has been interpreted to be clockwise (Abalos Vilaro, 1992; Ordoñes-Casado, 1998), which is characteristic of orogenic lode-gold deposits (e.g. Ridley *et al.*, 1997) and implies that rocks experience maximum pressures long before thermal maximum, and maximum temperatures are attained during a period of unloading (Bohlen, 1987).

LOCATION AND LOCAL GEOLOGY OF THE SÃO MARTINHO AND MOSTEIROS PROSPECTS

The São Martinho prospect occurs approximately 5 km east of Alter do Chão (Fig. 1C), south of the Blastomylonitic Belt. This area is approximately ellipsoidal in shape, defined from 2 km west of the São Martinho trigonometrical beacon to the railway cutting SE of trigonometrical beacon Travesso (Fig. 2) and has been extensively sampled on surface, trenched and drilled (25 boreholes, 6 of which were studied).

On surface the São Martinho area is mostly covered by a Palaeogenic eluvial deposit obscuring almost all of the surface outcrops of Proterozoic rocks with the exception of three outcropping windows of pale quartzites surrounding each trigonometrical beacon and other minor outcrops (Fig. 2). This cover is characteristically a carrier of free-gold grains derived from the Série Negra metasedimentary rocks (Oliveira *et al.*, 1997). There is little surface exposure of the Série Negra metasedimentary, intrusive, and extrusive metavolcanic rocks. However, pale grey and black quartzites, amphibolites, rhyolites, diabase/dolerite and weathered quartz-biotite schist can be observed in streams where the eluvial deposit is not developed or is thin enough to be washed away during the winter rains.

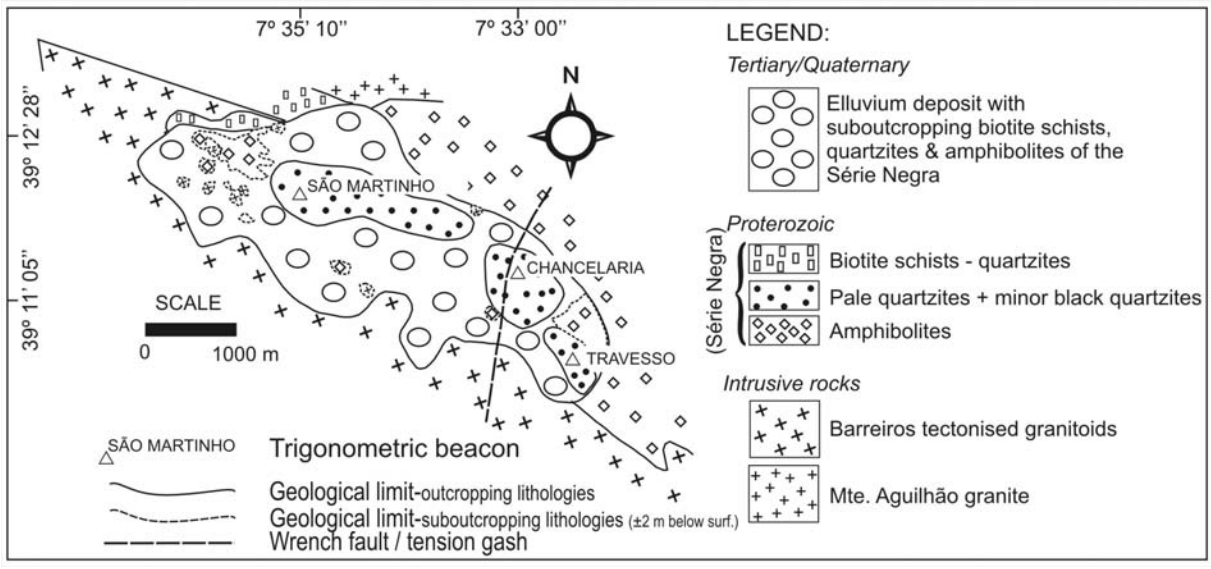

Figure 2: *Geological map of the São Martinho area interpreted from drilling the elluvium cover (adapted after fig.7 in De Oliveira et al., 1995). The map is a compilation of suboutcropping lithologies, e.g. amphibolites, biotite-schists-quartzites (Série Negra) and pods of the Barreiros tectonized granitoids, as well as poorly outcropping lithologies, e.g. amphibolites north of the elluvium cover and the Barreiros tectonized granitoids south of the deposit. The windows of pale grey quartzite occur in topographic highs.*

The São Martinho area characteristically comprises amphibolite-facies rocks and generally low gold grades throughout the area, although sporadic peaks in grade have been observed. This area typically consists of metapelites and meta-arenites of the Série Negra in the form of quartz-biotite schists and quartzites, amphibolites and banded amphibolites, together with granitoids, rhyolites, as well as basic dykes.

Quartz veins, microgranites and dolerite dykes are associated with regional, late Variscan, late Westphalian (Gonçalves *et al.*, 1978) wrench faults/fractures (Fig. 1C). The Mosteiros prospect (Fig. 1C) is a rectangular area orientated parallel to the regional strike that has been investigated with soil geochemistry, limited trenching and three boreholes; one of which was studied. In the Mosteiros area there remain a few additional large gold soil anomalies that have not been drilled and the northwest of the area remains open. The area comprises greenschist facies metasedimentary rocks of the Série Negra north of the Blastomylonitic Belt. The Série Negra is expressed as outcrops of folded black and pale grey quartzites and highly weathered and limonitized metapelitic (quartz-biotite schists) rocks. However, in contrast to São Martinho, this area is also characterized by metavolcanic rocks (tuffs) with intense Fe-carbonate (ferroan dolomite) alteration.

Host rocks to mineralization and styles of mineralization

The host rocks to mineralization at both São Martinho and Mosteiros are metasedimentary and metavolcanic rocks belonging to the Série Negra package. Gold grade normally occurs within one specific lithological unit or at the transition between two distinct lithological units as discussed below. At São Martinho, De Oliveira (2001a) has shown that gold grade in the area generally occurs very closely linked to the metapelitic quartz-biotite schists of the Série Negra or at the transition between amphibolitic-type lithologies (amphibolites/banded amphibolites) and these metasedimentary sequences. Locally, the amphibolitic-type lithologies also carry some gold. Furthermore, it has been noted that significant peaks in gold grade are typically associated with highly silicified zones at times with visible gold.

In the São Martinho area three styles of mineralization are evident:

(1) is relative to finely disseminated pyrrhotite in amphibolites and banded amphibolites;

(2) consists of veinlet-type mineralization that is aligned parallel or subparallel to foliation predominantly made up of pyrite, chalcopyrite (rare) and gold I, which is present within and on the margins of small quartz veinlets. These veinlets form part of an early generation of quartz (QI) that is probably emplaced by kinematic and metamorphic processes and occurs parallel or subparallel to the regional foliation (Fig. 3A) and which do not cross-cut the foliation. Where this foliation has since been folded the quartz veins are similarly folded such that parallelism of the veins with the regional foliation is maintained. Generally, QI veins are narrow, as observed in borehole core. This type of mineralization style is found mostly associated with amphibolitic-type lithologies as well as quartz-biotite schists; and

(3) consists of massive, blebby-type mineralization in quartz-biotite schist or on the edge of late quartz veins that cross-cut the foliation. At São Martinho, discrete, large and thicker quartz veins are frequently present (Fig. 3B). These quartz veins are designated QII and are later than quartz I since they cross-cut the regional foliation. QII veins occur up to 35 cm in thickness and commonly contain small enclaves of quartz-biotite schist and are

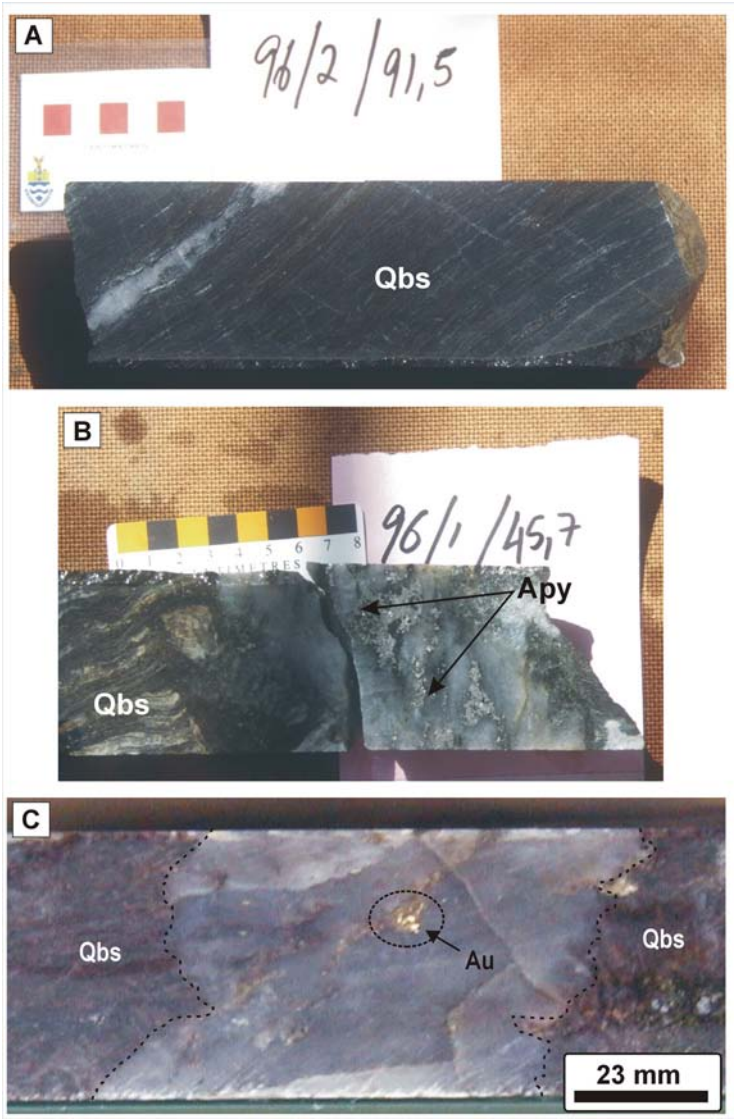

Figure 3: *São Martinho prospect. A- Foliation parallel quartz I (QI) veinlets in borehole POR96/2 (QBS – quartz-biotite schist); B- Foliation normal quartz II (QII) veins in borehole POR96/1 associated with massive arsenopyrite mineralization on its borders (Apy – arsenopyrite); C- Example of QII veins with visible gold in borehole POR97-10.*

associated with massive sulphide mineralization and visible gold (Fig. 3C). This mineralization style is commonly found in the quartz-biotite schist adjacent to these quartz veins and consists of masses of arsenopyrite intergrown with pyrrhotite, chalcopyrite, loellingite and gold II.

Gold grades in the Mosteiros prospect are low, averaging <1.5 g/t Au. Investigation of gold grade *versus* lithology type has shown that the gold grade is associated with the intensely carbonatized metavolcanic units (tuffs) and with interlaminated metavolcanic units and quartz-biotite schists. Breccia horizons of these same tuffs have been found to contain disseminated pyrite and also carry some gold.

Mineralization style at Mosteiros is best described as disseminated. This disseminated mineralization occurs both within the tuffaceous units and within the well-developed tuffaceous breccias in the area. The mineralization within the tuffs is restricted to macroscopic euhedral pyrite grains that range in size from < 1 mm to an average 2.0 to 2.5 mm, although

grains as wide as 7 mm have been documented (Inverno, 1995a). The tuffaceous breccias also contain smaller pyrite, rutile and very small arsenopyrite grains.

Mosteiros is also characterized by the development of two other microscopic ore minerals: (1) anhedral grains of ilmenite are common in trails parallel to regional foliation of the tuffs (ilmenite is also present as inclusions in the large pyrite grains); and (2) small (< 5 μm) euhedral arsenopyrite grains are disseminated throughout the gangue material.

MINERALOGY

São Martinho

Gangue mineralogy - The gangue mineralogy in the São Martinho area is restricted to the rock types described previously. Their major mineralogy is easily identified because of their larger grain size. Identification by optical microscopy, microprobe EDS/WDS and XRD has been undertaken.

The gangue mineralogy is dealt with in respect to the three rock units; basic (amphibolites/banded amphibolites), metapelitic (quartz-biotite schists) and meta-arenitic (quartzites) rock units. Amphibolites are composed of quartz, magnesiohornblende-actinolite, oligoclase-andesine-labradorite-bytownite, while the banded amphibolites comprise magnesiohornblende-tschermakite, andesine-labradorite-bytownite (De Oliveira *et al.*, 2003c). In both rock types tremolite, kaersutite (rare), pargasite/edenite, epidote, wollastonite, omphacite, graphite, kutnahorite, hydroxyl-apatite, monticellite, chiolite and tephroite have also been identified by XRD techniques.

The metapelitic portion of the Série Negra, the quartz-biotite schists, consist mainly of quartz, biotite and rare muscovite and have as accessory minerals calcite, chlorite (ripidolite-brusnvigite), tourmaline, garnet, monticellite*, chloritoid*, pseudobrookite*, ferroan dolomite*, charlesite*, wollastonite*, sillimanite*, chiolite*, illite*, sapphirine*, ettringite* (*-identified by XRD) and monazite (identified using EDS).

Muscovite mica (Fig. 4A) is common only in a small number of samples close to mineralized zones. This muscovite seems to be derived from the discoloration of biotite and in many instances the muscovite is in optical continuity with biotite. Muscovite is often seen bent, indicating that tectonism was active during its formation. Common to the quartz-biotite schist horizons at São Martinho are large porphyroblasts of almandine garnet. These porphyroblasts are unrotated and thought to have grown late within the gangue paragenetic sequence with the exception of quartz (Fig. 5), since the gangue mineral surrounding garnet are aligned and stretched by the intervening schistosity developed.

Chlorite occurs both as an alteration product of biotite and rimming pyrite II veinlets (Fig. 4B) in the first mineralization stage (RS I, see later). Very small tourmaline grains that can easily be confused with amphibole are scattered throughout the quartz-biotite schist (e.g. Fig. 4C) especially near mineralized fractures/veinlets. Very small, disseminated albite grains are, at times, more or less abundant close to pyrite II veinlets when they are present.

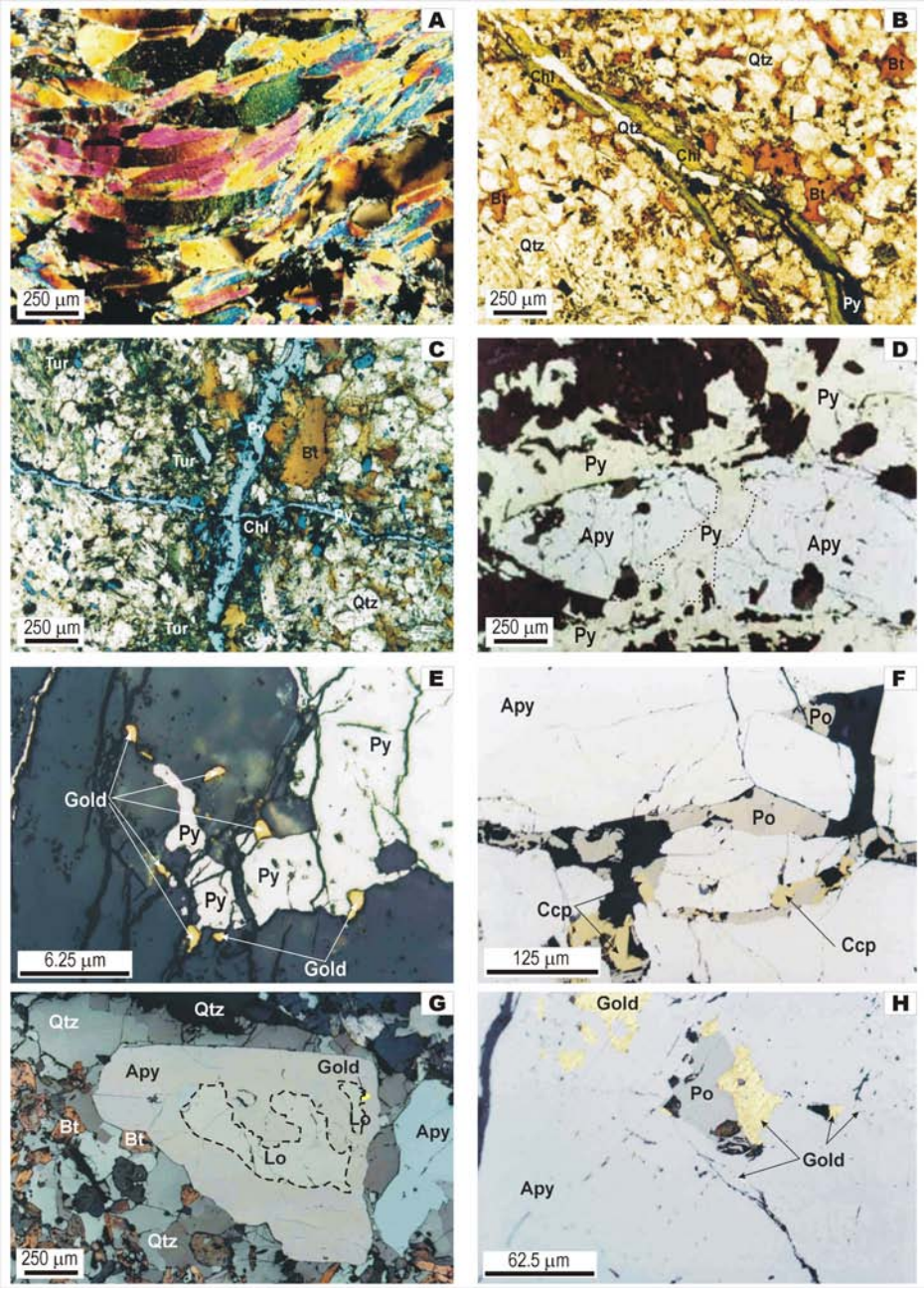

Figure 4: *Selected examples of the gangue and ore mineralogy from the São Martinho prospect. A- Bent muscovite laths (POR97-10-42, cross-polarized transmitted light); B- Pyrite II veinlet with chlorite (Chl) rim (SP6-16, plane-polarized transmitted light), Bt - biotite; C- Pyrite I (horizontal) and pyrite II (vertical) veinlets with chlorite (Chl) alteration haloes as well as hornblende and tourmaline (Tur) (SP6-16, plane-polarized transmitted and reflected light), Bt – biotite, Qtz - quartz; D- Arsenopyrite (Apy) I pod (stretched) cut by pyrite (Py) II veinlet (dashed). Grains such as these have inclusions of gold I (SP6-19, plane-polarized reflected light); E- Pyrite II grain with gold I infilling fractures (SME-1023, plane-polarized reflected light); F- Late fractures in arsenopyrite II (Apy) filled with chalcopyrite II (Ccp) and pyrrhotite II (Po) (POR96-1-7, plane-polarized reflected light); G- Arsenopyrite II (Apy) grain within quartz-biotite schist. This arsenopyrite encloses a large loellingite (Lo) grain that has a small speck of gold in contact with it [POR96-1-11, cross-polarized (@ 20º) reflected and transmitted light]; H- Gold II adjacent to pyrrhotite II and in late fractures (e.g. fracture at SE section of image). Both pyrrhotite and gold are enclosed by arsenopyrite II (POR96-1-7, plane-polarized reflected light). Mineral symbols after Kretz (1983).*

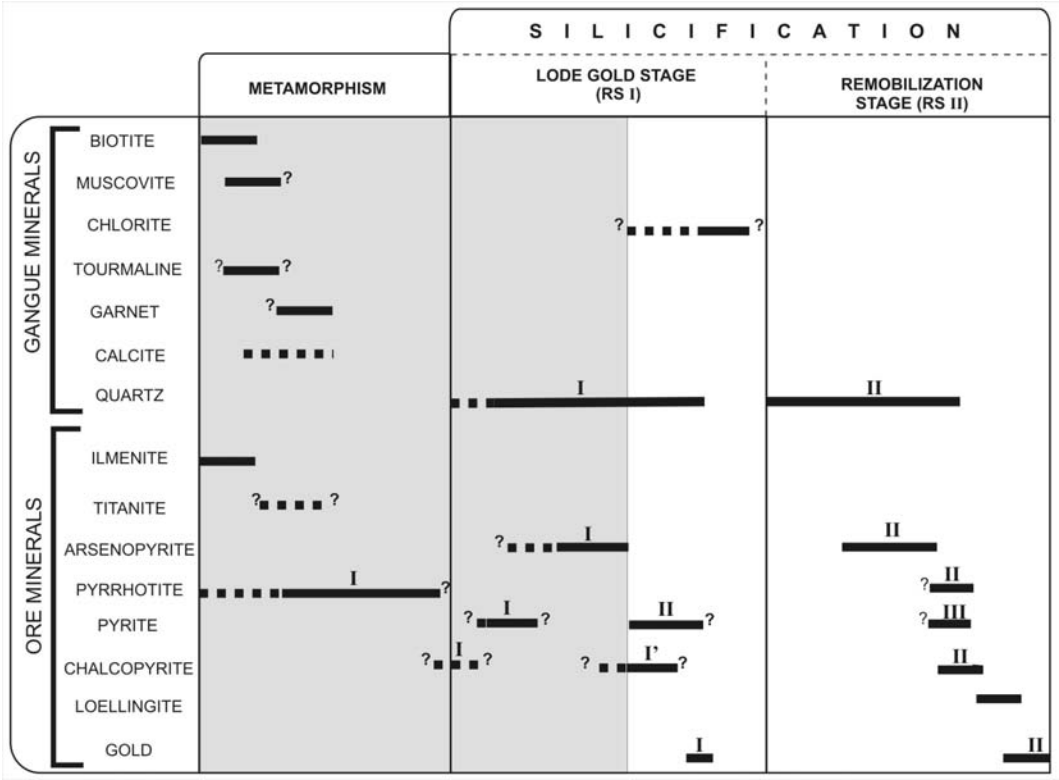

Figure 5: *Paragenetic sequence for the gangue and ore minerals in the São Martinho prospect. The shaded area represents the probable window of active tectonism as derived from the observation of the form and habit of the gangue and ore minerals.*

Alteration assemblages – The products of silicification, chloritization and muscovitization/sericitization are easily recognised at São Martinho. However, some of the alteration assemblages are subtle and difficult to recognize in the metasiliciclastic and metavolcanic rocks of the Série Negra area (namely, tourmalinization and albitization, due to the very small size of the grains, and carbonatization).

Ore mineralogy and paragenetic sequence - The paragenetic sequence of the ore minerals in the São Martinho area must take into account both gangue and ore minerals formed while metamorphism and tectonism were active. The paragenesis at São Martinho is broadly summarized in to two silicification events that form part of two distinct mineralizing events: (1) a lode gold stage denoted as RSI; and (2) a remobilization stage denoted as RSII (Fig. 5). Quartz-biotite schists have a strong schistosity developed as a result of interlayered quartz-rich and biotite-rich layers. These quartz-biotite schists are, at times, interlayered with amphibolitic-type (amphibolites/banded amphibolites) lithologies. The quartz-biotite schist layers have a Ti-bearing mineral (ilmenite) that occasionally is rimmed with titanite. This ilmenite is aligned parallel to the foliation in the rocks and is thought to have originated from the sedimentary protolith of the quartz-biotite schist. Alignment is due to shearing and flattening and the coating of ilmenite by titanite is due to the reaction with calcium. The amphibolites have accessory titanite, but little ilmenite.

The coating of ilmenite by titanite in quartz-biotite schists implies a later appearance of titanite. Since titanite occurs almost exclusively in the amphibolitic-type lithologies, the titanite must have been introduced after generation of the amphibolitic lithologies.

The banded amphibolites and amphibolites have finely disseminated pyrrhotite I mineralization, which due to their alignment along bands parallel to the amphiboles were likely formed during metamorphism (Fig. 5), as well as minor chalcopyrite I. Chalcopyrite I appears both as finely disseminated mineralization in the amphibolites or as inclusions (Ccp I'?) within the disseminated pyrrhotite. The lack of textural relationships between these two ore minerals precludes the exact chronological placement in Figure 5, of their time-lines with relation to each other. However, it would appear that there are two generations of chalcopyrite developed up to the end of the gold I mineralizing event, RSI (Fig. 5), one (Ccp I) approximately coeval with disseminated pyrrhotite I in amphibolites/banded amphibolites, as inclusions, and a later one (Ccp I') (Fig. 5). The Série Negra rocks also show evidence of silicification with the introduction of quartz I veins, which are parallel to the foliation and have been described previously.

The mineralization style during stage RS I (Fig. 5), is best described as disseminated, although some aspects of it are veinlet-type. RS I introduced pods of arsenopyrite I that were sheared and stretched and aligned parallel to the foliation (Fig. 4D) while tectonism was active in the region. Associated with RS I are pyrite I veinlets that occur subparallel to the foliation and which were subsequently cut by pyrite II veinlets (Fig. 4C). Pyrite I veinlets were probably introduced before arsenopyrite I. However, in all the samples studied, no clear, unequivocal cross-cutting relationships between arsenopyrite I and pyrite I were observed and their sequential relationship as shown in Figure 5 is a tentative approach. However, the introduction of gold I is clearly associated with pyrite II veinlets (Fig. 4E) that have cut across the arsenopyrite pods (Fig. 4D). Pyrite II is undeformed, hence, at the time of pyrite II introduction, tectonism was no longer active in the shear zone. Gold I is also deposited as tiny grains (< 2 μm) in the (stretched) arsenopyrite I pods adjacent to the pyrite II veinlets that cross cut these arsenopyrite I grains. Only a few gold grains that can be clearly attributed to this stage of mineralization were observed in thin section.

Disseminated chalcopyrite I' grains are also found with arsenopyrite and pyrite grains of RS I, but they show no cross-cutting relationships. Adjacent to the pyrite I veinlets, a thin (< 0.5 mm) chlorite rim around quartz I is evident in a few samples. Commonly, QI thinly envelops the pyrite I veinlets.

A second mineralising event (RS II), linked to renewed silicification (QII) occurs and overprints RS I. This second event is characterised by quartz II (QII) veins that cut across the foliation of the Série Negra metasedimentary rocks and massive-style mineralization. This second silicification event is characterized by arsenopyrite II, pyrite III, chalcopyrite II, pyrrhotite II, loellingite (high temperature mineral) and gold II.

Quartz II veins have, at times, visible gold, pyrrhotite and arsenopyrite associated with them. Chalcopyrite II and pyrrhotite II are found in-filling late fractures in the arsenopyrite II and are a distinguishing feature of RS II (Fig. 4F). In a few grains of arsenopyrite II there are also pyrite-filled fractures. This pyrite is interpreted as pyrite III, but its occurrence is rare. Loellingite has not been found as isolated grains, but only as inclusions in arsenopyrite II (Fig. 4G), which supports its crystallization after arsenopyrite II (e.g. Clark, 1960) (Fig. 5). Gold (II) is more abundant in this stage than in RS I, although in cases it is very fine, and has always been observed or enclosed by or rimming loellingite (Fig. 4G) and in-filling late fractures in arsenopyrite II (Fig. 4H). Hence, gold II is late with respect to the rest of the paragenetic sequence (Fig. 5).

Ore mineral chemistry – Chemical analyses of the ore and gangue minerals was carried out using a Jeol Superprobe 733 with 4 WDS spectrometers (8 crystals), Link eXLII and Link Lemas automation system, Oxford/Link SiLi detector for EDS work and SIS ADDA image capturing system with analySIS image analysis package, at the University of Pretoria. It can be stated with some certainty that based on the analyses of the São Martinho ore minerals, pyrite, arsenopyrite and gold, apart from the latter, do not differ significantly in terms of their chemistry from RS I to RS II mineralizing stages (Table 1). Only pyrrhotite II was analysed given the similar results obtained previously for the other generations of ore minerals.

Table 1. Average microprobe data for the ore minerals analysed in São Martinho. All values in wt%; 20 nA beam current; 15 kV accelerating voltage; 5 µm beam diameter; 40s (peak) and 20s (background) counting times; max. error is ± 5% for major elements

	Pyrite I	**Pyrite II**	**Pyrite III**	**Chalco-pyrite I**	**Chalco-pyrite II**		**Pyrrhotite II**
	(n=3)	*(n=23)*	*(n=3)*	*(n=10)*	*(n=3)*		*(n=23)*
S	53.65	53.50	52.02	32.65	34.43	**S**	39.37
Fe	46.29	45.95	47.28	29.88	30.61	**Fe**	59.54
Co	0.05	0.03	0	0.03	0.01	**Co**	0
Ni	0	0.13	0.06	0.02	0.01	**Ni**	0.05
Cu	0.01	0.07	0	35.40	34.00	**Cu**	0.02
As	0.08	0.04	0	0.01	0.05	**As**	0.04
Ag	0.02	0.02	0.02	0.01	0.03		
Au	0.03	0.01	0.02	0	0.01		

	Arseno-pyrite I	**Arseno-pyrite II**		**Gold I**	**Gold II**
	(n=7)	*(n=26)*		*(n=2)*	*(n=19)*
S	18.94	18.14	**S**	0.04	0
Fe	33.37	34.29	**Fe**	0.03	1.00
Co	0.14	0.06	**Co**	0	0
Ni	0.08	0.13	**Ni**	0.01	0
As	46.54	47.22	**Cu**	0.01	0
Au	0.01	0.01	**As**	0	0
			Ag	7.62	15.00
			Au	88.35	84.12

Pyrite I, II and III - There are no salient characteristics to distinguish between any of the three generations of pyrite using the element suite S, Fe, Co, Ni, As, Ag, Au for analysis (Table 1). Fluctuations in the amount of Fe and S occur in all three pyrite types and the deviation, in the order of 1%, is not sufficient to attribute any significance to it. Minor elements such as Co, Ni, Au and Ag do not indicate any significant differences.

Arsenopyrite I and II - Analysing the data for the two generations of arsenopyrite shows that there is virtually no difference between them. They are both high in sulphur (Table 1); on the limit permitted by stoichiometry, and on occasions show traces of Au, Co and Ni.

Gold I and II - In São Martinho, two gold generations have been identified (Fig. 5) associated with RS I and RS II, respectively. These two generations of gold are clearly identified in terms of the gold chemistry. Gold I associated with pyrite II is $Au_{88.35}$ (Table 1) with approximately 7.5% Ag and traces of S, Cu, Ni and Fe. Gold II is $Au_{84.12}$ (Table 1) with a significant amount of Ag (average Ag_{15}). Gold II also shows traces of Ni, Fe, and As. However, the gold content of a few individual, undoubtedly gold II grains, show similar analytical data to gold I grains.

Mosteiros

Gangue mineralogy – In the one borehole studied (SP2), gangue minerals in Mosteiros were difficult to identify fully due to their very small grain size in the tuffaceous host rocks apart from minerals such as quartz, carbonates (Fig. 6A), muscovite (Fig. 6B) and fuchsite (Fig. 6C). Even with the microprobe, identification of individual minerals is difficult because the tuffs are highly altered with the development of pervasive ferroan dolomite. Using XRD techniques, four samples of carbonatized tuffs and breccias from mineralized horizons were investigated in borehole SP2. The obtained spectra were compared to known published powder diffraction standards.

Samples near the top of the borehole gave spectrum peaks that correlate well for quartz, ferroan dolomite (Fig. 6A), dravite (Mg-tourmaline), wollastonite, goethite, dolomite, brookite, ilmenorutile, kyanite and sillimanite. Spectra with poorer correlation were obtained for perovskite, bixbyite and zoisite. Optical microscopy and microprobe work revealed the presence of copious quantities of fine, blue and yellow mica (muscovite/sericite) as well as finely disseminated chlorite.

In deeper levels of the borehole, X-ray spectra from the brecciated horizons show the mineralogy to consist mainly of quartz, ferroan dolomite, dolomite, graphite and ulvospinel. Accessory mineralogy consists of sphalerite (not observed in the course of this study) clinozoisite, ilmenite, ilmenorutile, eskolaite, fuchsite (Inverno, 1995b), cuprite and jacobsite.

Alteration assemblages - At Mosteiros, given the gangue mineralogy observed, three distinct alteration assemblages are recognised. These include:

(1) products of pervasive carbonatization (e.g. Fig. 6A);
(2) products of muscovitization (e.g. Fig. 6B); and
(3) silicification, which occurred during a prominent late brecciation stage in the Mosteiros area.

The products of fuchsitization are also common (Fig. 6C), as are those of chloritization.

Ore mineralogy and paragenetic sequence - The ore mineral assemblage is mostly grouped in a brecciation stage while the prominent alteration assemblage minerals are largely grouped in an earlier synmetamoprhic stage (Fig.7).

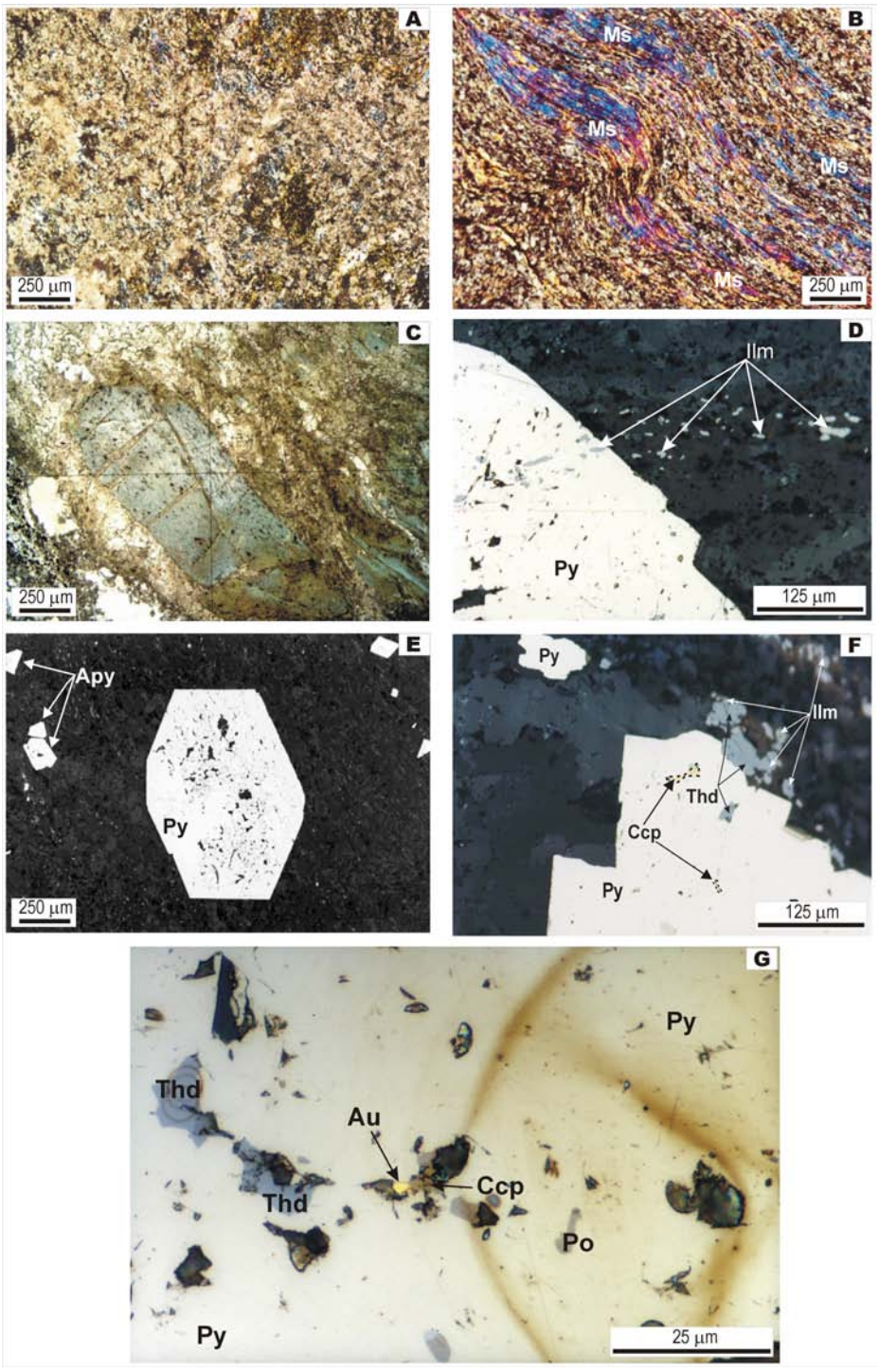

Figure 6: *Photomicrographs of aspects of the gangue and ore mineralogy from the Mosteiros prospect. A- Pervasive ferroan dolomite alteration (light colours) (SP2-28; cross-polarized transmitted light); B- Muscovite in carbonatized tuffs (SP2-39; cross-polarized transmitted light); C- Coarse fuchsite (Cr-rich muscovite) in sample SP2-2 (plane-polarized transmitted light); D- Trails of ilmenite (Ilm) carrying through a large euhedral pyrite grain (SP2-11; reflected light); E- Photomicrograph of euhedral pyrite grains in a matrix of carbonatized tuff (reflected light; 5x) and disseminated arsenopyrite; F- Chalcopyrite (Ccp) and tetrahedrite (Thd) inclusions in pyrite. Tetrahedrite and ilmenite are also observed bordering the pyrite (SP2-30; reflected light); G- Sample SP2-12 showing gold (Au) adjacent to chalcopyrite. Tetrahedrite and pyrrhotite inclusions can be seen nearby (brown circles are microprobe marks; reflected light). Mineral symbols after Kretz (1983) except for tetrahedrite (Thd).*

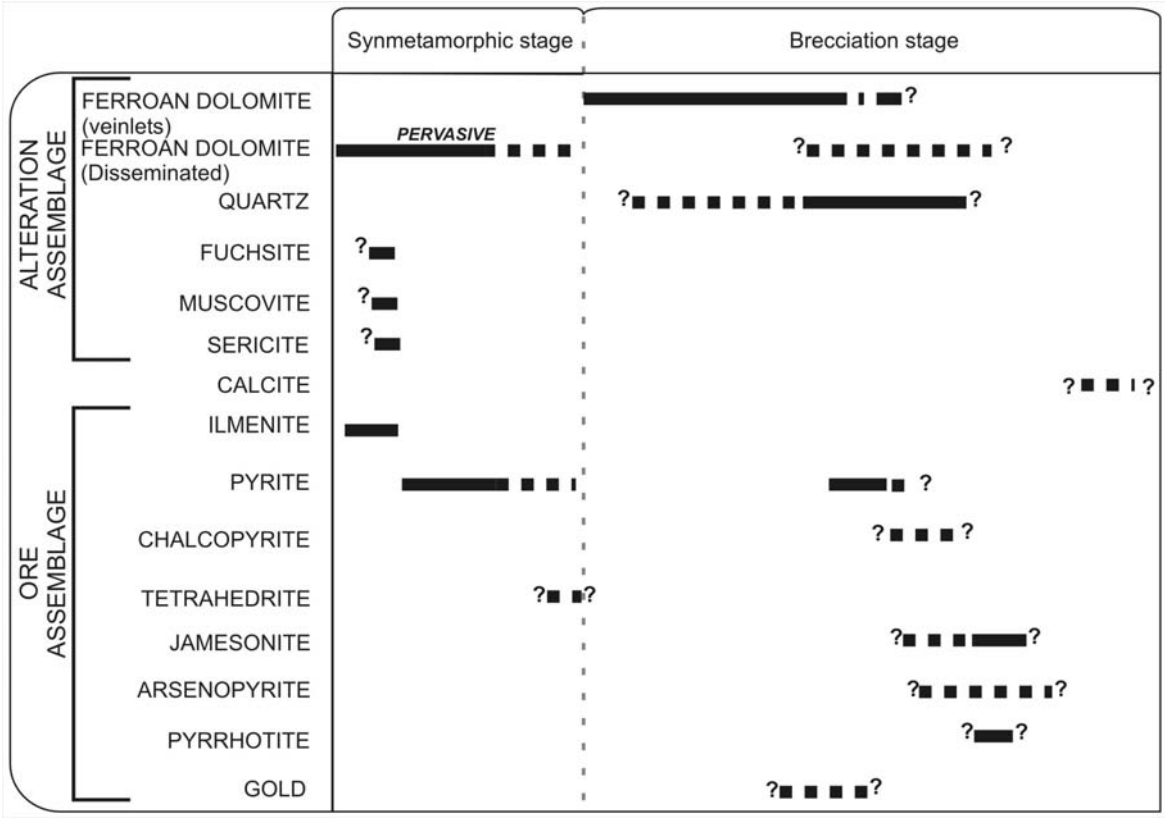

Figure 7: *Paragenetic sequence for the alteration and ore minerals in the Mosteiros area.*

The metallic ore minerals identified at Mosteiros are ilmenite, pyrite, arsenopyrite, chalcopyrite, tetrahedrite, pyrrhotite, gold and jamesonite. Ilmenite is observed in belts (trails) trending parallel to the foliation of the tuffaceous rocks. These trails in places can be traced through pyrite grains (Fig. 6D) although the spongy centres of the pyrite make this difficult to observe clearly. The euhedral pyrite, therefore postdates the development of ilmenite.

Two generations of pyrite are identified: (1) large euhedral, rarely subhedral (when embayed), pyrite grains with atypical sections that were recrystallized during metamorphism; and (2) very small, disseminated, cubic section pyrite grains. Large euhedral pyrite grain sections at Mosteiros are not “cubic” or four-sided, but can range from pentagonal through octagonal-shaped (e.g. Fig. 6E). Pyrite grains are large, averaging 2 mm across, although exceptional cases of 7 mm have been recorded (e.g. Inverno, 1995a). Pyrites are typically spongy in the core and are rimmed (overgrown) by more compact euhedral pyrite (Fig. 6E). Near surface, meteoric water circulation has virtually replaced the pyrite grains with an Fe-oxide phase, probably goethite.

Arsenopyrite was observed as small (3-5 µm) euhedral grains within the gangue or rarely as larger grains adjacent to subhedral pyrite grains (Fig. 6E). No textural relationships for determination of accurate timing of their crystallization were observed.

Chalcopyrite occurs as very small, irregular-shaped inclusions within the large euhedral and subhedral pyrite grains (Fig. 6F). These inclusions in pyrite have been found to measure < 7 µm across. No discrete chalcopyrite grains have been found in the gangue (i.e. outside the pyrite grains). The lack of clearly identifiable textural relationships between the pyrite and chalcopyrite precludes the determination of the accurate timing of chalcopyrite

mineralization. However, one sample from borehole SP2 showed a fine (< 0.5 µm-wide; 3 µm-long) crack in the large euhedral pyrite that was apparently filled with chalcopyrite, which implies a later growth of the chalcopyrite in relation to the pyrite.

Common alteration processes of the Mosteiros rocks were brecciation and silicification. This brecciation resulted in the successive injection of ferroan dolomite and quartz in veinlets that caused the break-up of previously pervasively carbonated (ferroan dolomite) tuffaceous material as well as the break-up of large euhedral pyrite grains. Therefore, the pervasive carbonate alteration, which is so characteristic of the Mosteiros rocks was possibly earlier than, or contemporaneous with, metamorphism and has taken place before the onset of silicification (Fig. 7).

Pyrrhotite is rare (less common than chalcopyrite) and is observed as small round inclusions in large euhedral pyrite grains (Fig. 6G). Tetrahedrite was observed as very small (up to 4 µm across) anhedral, subrounded inclusions within the large euhedral pyrite grains (Fig. 6G). No textural relationships were observed that allow for an accurate genetic time sequence of this mineral and hence a dashed line shows its placement in Figure 7.

Jamesonite, found only in one sample as crack-fill material in one large subhedral pyrite, is identified as introduced late in the paragenetic sequence, probably linked with brecciation and silicification.

Carbonate *(s.l.)* veinlets are common in Mosteiros. Carbonate related to ore minerals seems to be of two distinct types: (1) pervasive, finely disseminated ferroan dolomite; and (2) ferroan dolomite veinlets that break up large euhedral pyrite grains.

Muscovite (+ sericite) is also commonly found in the rocks of the Mosteiros area. Muscovite developed prior to the introduction of pyrite as clusters of fine euhedral pyrite grains, and was seen cutting trails of muscovite. Fuchsite, commonly visible to the naked eye is believed to crystallize with muscovite because these are often observed parallel to each other and no cross-cutting relationships have been observed.

Quartz was introduced during the brecciation stage, firstly as discrete veinlets and, secondly, as veinlets that occupy previously formed ferroan dolomite veinlets. At least three generations of quartz veinlets have been identified; the latter of which is only visible under cathodoluminescence (CL) conditions. There is a decrease in veinlet thickness from the earlier to the latter generations. Generally, the earlier quartz veinlets are <1 mm-wide and the latter, CL visible, quartz veinlets are in the order of 5-9 µm. However, only the first one, which creates the thickest veinlets, seems to be associated with sulphide mineralization. Microscopic quartz veining is common in rocks from this area. The pervasive carbonatization has, at least macroscopically, obliterated almost all the quartz veinlets. Calcite veinlets (< 30 µm across) are common in the thin sections studied. These are late with respect to sulphide mineralization (Fig. 7) and cut across pyrite grains.

In this area, microscopic gold particles have only been observed in three samples out of a total of 39 samples that were studied microscopically. In one sample, a gold grain smaller than 2 µm has been observed in tuffaceous gangue adjacent to two euhedral pyrite grains and partly surrounded by tetrahedrite. A very small gold grain (~1µm across) has been observed in another sample adjacent to chalcopyrite within pyrite (Fig. 6G). The third gold grain was observed outside pyrite mineralization, in a brecciated horizon of carbonatized tuff. In this sample, gold was a large (1.6 mm-long), L-shaped grain with disseminated pyrite. No textural

relationships were identified that allows accurate placement of gold in the paragenetic sequence. However, since it has been found associated with the brecciation stage it is thought to be "late" in the paragenetic sequence after the development of tetrahedrite (Fig. 7).

Mosteiros gold chemistry - The almost total lack of (microscopically observable) auriferous mineralization in this area, initially steered one toward the possibility of invisible-type mineralization, i.e. "invisible gold" (e.g. Kojonen and Johanson, 1997; Ashley *et al.*, 2000). The gold grade, although low, was present in definite horizons that were scrutinized and sampled. However, no gold grains, apart from the three already referred to, were found.

The small grain size of the constituent mineral phases is a factor that hampers conventional identification by optical microscopy. Hence, to avoid missing any mineral phase with characteristic elements, backscattered electron element maps were made, from rim to core, of both euhedral pyrite and arsenopyrite grains. Element maps of the euhedral pyrite grains show the occurrence of S and Fe, Sb (as small inclusions), traces of Cu, Ni, and Ag and a strong signature for Au (fig. 4 in De Oliveira, 2003). The element maps of the arsenopyrite grains also indicate the presence of S, Fe, and As, as well as traces of Cu, Ni, Co, Ag (Fig. 8), but these qualitative indications are not supported by quantitative microprobe analyses (Table 2). Nevertheless, the presence of Au in this fashion probably occurs in the crystal lattices of pyrite and arsenopyrite (i.e. as invisible gold).

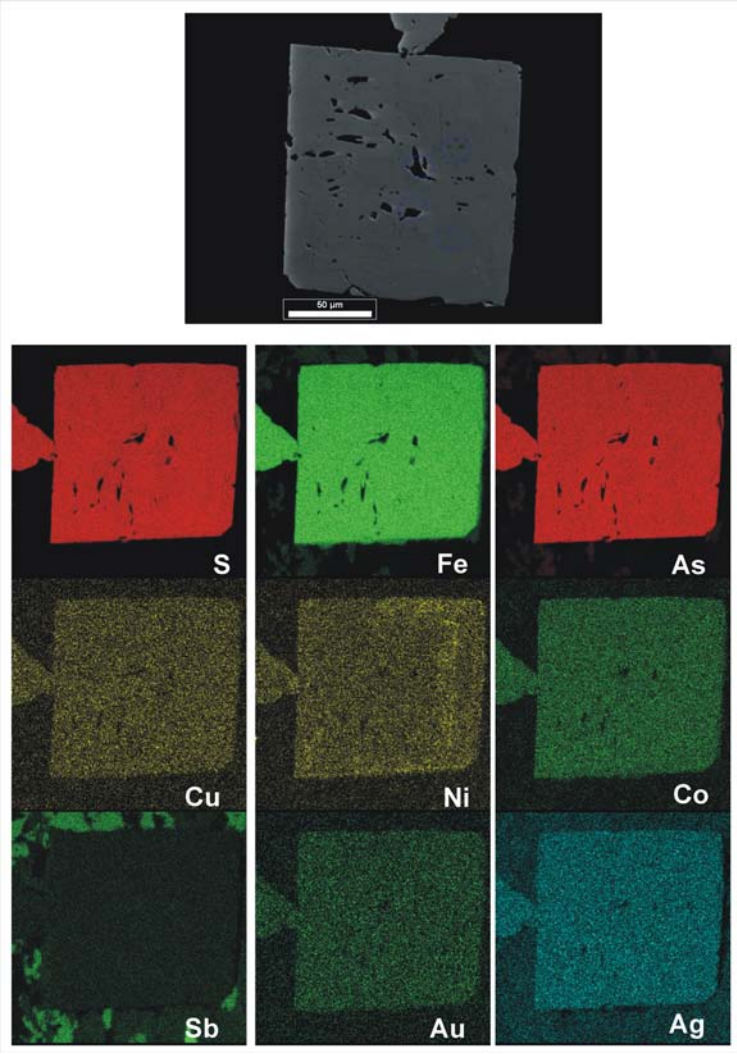

Figure 8: *Backscattered element maps of euhedral arsenopyrite from the Mosteiros prospect.*

Table 2. Average microprobe data for the ore minerals analysed in Mosteiros. All values in wt%; 20 nA beam current; 15 kV accelerating voltage; 5 µm beam diameter; 40s (peak) and 20s (background) counting times; max. error is ± 5% for major elements

	Euhedral pyrite n=13	Arsenopyrite n=14	Tetrahederite n=3	Pyrrhotite n=6	Chalcopyrite n=5	Gold n=6
S	53.17	23,21	25.75	38.62	37.55	0.02
Fe	45.84	35,22	7.78	55.67	33.60	0.14
Co	-	-	0.02	0.10	0.03	0.01
Ni	0.05	0,06	0.01	0.09	0.01	0.01
As	1.17	41,32	1.40	0.02	0.02	0.03
Cu	-	-	34.00	0.26	28.89	0.01
Sb	-	-	24.81	-	0.01	0.04
Au	0.02	0,00	0.04	0.02	0.05	98.58
Ag	-	-	0.87	-	0.01	0.02

Six microprobe analyses (Table 2), carried out on the only gold grain big enough for analysis, revealed that this gold grain contained ranges in gold from $Au_{96.36}$ to $Au_{99.47}$ (average $Au_{98.6}$) and negligible amounts of Ag, Cu and Fe (across its entire surface).

FLUID INCLUSIONS

Published fluid inclusion data (De Oliveira *et al.*, 2001a, b; De Oliveira *et al.*, 2002b) for these areas show that there are few if any preserved primary fluid inclusions available for study in quartz grains and the available secondary inclusions in the same grains are mostly small and on the limit suitable for study. However, since the secondary fluid inclusion population are mostly grouped in planes parallel to gold mineralized fractures, this indicates that they most likely represent the primary mineralizing fluids (Fig. 9A).

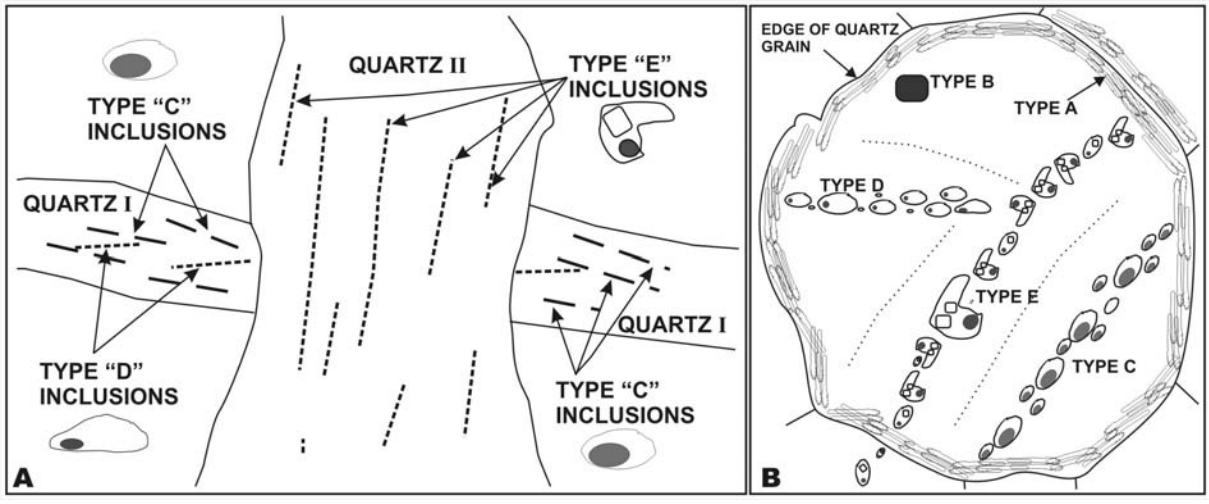

Figure 9: *A- Idealized cross section through quartz I and quartz II veinlets and veins, respectively, in the São Martinho area. Dashed lines indicate FIP's of the various types of fluid inclusions (C to E only) and show the parallel nature of the FIP's with respect to veinlet/vein edges. These orientations are parallel or subparallel to mineralization in a significant number of cases. B - Idealized quartz grain showing the various types of fluid inclusions observed in samples from the São Martinho area. Inclusions are not to scale both within types and between types.*

At Mosteiros there was no fluid inclusion microthermometry undertaken due to the unsuitability of the material, given the very small size of the fluid inclusions contained therein. At São Martinho, 5 types of fluid inclusions (Fig. 9B) are recognized in quartz crystals, although type A refers to stretched/leaked primary inclusions lining the borders of quartz grains and for which no microthermometric data were obtained. The microthermometric data are summarized in Table 3.

Table 3. Summary of the microthermometry results obtained in the São Martinho prospect. (*) Does not include 22 measurements > 550 ºC; all results are median temperatures. Temperature expressed in ranges and average (in brackets). n= number of inclusions (adapted after De Oliveira et al., 2002b)

Mineralization stage	Fluid inclusion type	Microthermometric results (ºC)							
		Tm_{CO2}	$Th_{CO2(L)}$	$Th_{CO2(V)}$	Te	Tm_{ice}	Th_{tot}*	$Th_{(L)}$	Tm_{dau}
?	Type B (CO_2)	-60	-0.9 to +7	-	-	-	?	-	-
Stage 1 (RS I)	Type C (H_2O-NaCl -CO_2-CH_4)	-71 to -60 (-64.1, n=20)	-	-21 to +7 (+2.3, n=18)	-	-	245 to 521 (371, n=28	-	-
	Type D (H_2O-NaCl)	-	-	-	-52.6 to –38.7 (-41.7, n=72)	-13 to +1.3 (-3.6, n=74)	-	112 to 212 (129, n=76)	-
Stage 2 (RS II)	Type E (H_2O-NaCl) Hypersaline	-	-	-	-	-	-	120 to 470 (290, n=161)	290 to >550 (400*, n=131*)

The fluid inclusion data indicate the presence of lower temperature fluids (H_2O-CO_2-CH_4-NaCl) associated with QI veinlets and higher temperature fluids (hypersaline, magmatic) associated with QII veins. The data from São Martinho indicate that the mineralizing fluids associated with RS I are generally dilute brines additionally containing CO_2 and CH_4. The fluids can contain up to 76 mole % CO_2 and salinities vary from 0.5 to 17.2 wt% NaCl equivalent (types C and D), whereas salinity values of between 32 and 62 wt% NaCl equiv. have been estimated for Type E hypersaline fluid inclusions (De Oliveira *et al.*, 2001a, b; De Oliveira *et al.*, 2002b).

Trapping pressures were estimated using calculated isochores and an independent geothermometer. The independent geothermometer used was the formation temperature of hydrothermal chlorite associated with pyrite II veinlets that yields temperatures between 336 and 400 ºC (see later).

Since fluid inclusion types C and D are associated with the early stage of mineralization (RS I), i.e. a syntectonic mineralization stage, and the calculated isochores already take into

account estimates of fluid density and salinity, with estimated pressure of trapping read off from graphs of pressure *versus* temperature. For this purpose, a mean temperature of 368 ºC, which for type C fluid inclusions is very close to the median temperature (371 ºC), but for type D inclusions it is way off the median (129 ºC), was used. Results show that the estimated trapping pressures would be approximately between 4.3 and 6.2 kbar using the mean although when using ± 1x std. dev., pressures vary from 3.8 to 7 kbar, which conform to other published results for the Série Negra (e.g. Abalos *et al.*, 1991a, b).

GEOTHERMOMETRY

The partitioning of elements between two mineral phases is a particularly useful method because it is a temperature dependant phenomenon that is independent of the activity of volatile components (CO_2 and H_2O) in the geological environment (Ferry and Spear, 1978). Here, due to the suitability of samples only data from São Martinho is presented.

The geothermometry results obtained from chlorite (Cathelineau, 1988) haloes around some pyrite II veinlets and garnet-biotite (Ferry and Spear, 1978) pairs are shown in Table 4. The calculated temperatures of formation vary between ~325 and ~400 ºC for chlorite and ~574 and ~591 ºC for garnet-biotite. In the case of the garnets studied, these are Alm80 (approximately) and the temperatures, close to 600 ºC, correlate well with the amphibolite facies metamorphic field (at approximately 5 kbar) (e.g. see fig. 4-1 in Winkler, 1979 and fig.1-11in Turner, 1981).

The arsenopyrite geothermometer is based on the composition of arsenopyrite as a function of temperature and pressure in each of the assemblages surrounding arsenopyrite (Kretschmar and Scott, 1976). The occurrence of these mineral phases, namely arsenopyrite II, pyrrhotite II and loellingite, in contact with each other in the RS II mineralized veins at São Martinho, make this geothermometer suitable for use. Individual analyses (not discriminated in Table 1) of arsenopyrite II that met this requirement were used to calculate probable formation temperatures that vary between 371 to 642 ºC.

SULPHUR ISOTOPES

In the course of this study 6 samples for S-isotope investigation were collected, one from the Mosteiros area and the remainder from the São Martinho area.

Sample descriptions and results obtained

A brief description of the borehole samples from which the sulphide minerals, namely pyrite, pyrrhotite and arsenopyrite, were extracted for S-isotope measurements ($\delta\ ^{34}S$ values) are shown in Table 5, together with the obtained data.

Discussion of obtained $\delta\ ^{34}S$ values

In the Mosteiros and São Martinho prospects the $\delta\ ^{34}S$ values obtained for all the sulphide samples range from -3.0 to -6.5 ‰. The $\delta\ ^{34}S$ values are, however, not sufficiently close to zero to indicate solely a magmatic source of S. The S-isotope record (Schidlowski, 1988) shows the sulphide $\delta\ ^{34}S$ value curve to be negative from about 0.7 Ga to the present. A graphical estimate, using Schidlowski's curve, has been made for the approximate $\delta\ ^{34}S$ values around 340-315 Ma; the postulated timing of mineralization in this area (see later),

which yields negative δ ^{34}S values of between -3.0 and -8.0 ‰ (fig. 6.24 in De Oliveira, 2001a).

Table 4. Analytical results used for calculation of formation temperatures of chlorite and garnet-biotite from São Martinho. (*) Computed by the Cathelineau (1988) method and (**) by the Ferry and Spear (1978) method. Bt= biotite; Grt= garnet

		6-16	6-16-1	6-19	6-19a	6-7	6-12	Results
Chlorite (*)	SiO_2	27,63	27,74	28,05	27,42	25,52	26,27	
	Al_2O_3	9,78	9,25	8,76	9,82	10,24	9,25	
	TiO_2	0,00	0,00	0,02	0,01	0,02	0,01	
	FeO	40,47	42,04	41,24	40,97	38,69	37,92	
	MnO	0,14	0,13	0,08	0,18	0,26	0,11	
	MgO	5,72	5,44	6,07	5,64	4,61	5,25	
	CaO	0,13	0,17	0,18	0,13	0,12	0,14	
	Cr_2O_3	0,06	0,00	0,00	0,01	0,02	0,00	
	NiO	0,00	0,00	0,00	0,00	0,00	0,00	
	Na_2O	0,11	0,02	0,06	0,04	0,06	0,06	
	K_2O	0,05	0,06	0,06	0,06	0,01	0,02	
	Total	84,08	84,85	84,53	84,28	79,54	79,03	325.1
	Structural Formula (23 O)							to
	Si	6,70	6,73	6,80	6,66	6,57	6,76	399.0
	Al (IV)	1,30	1,27	1,20	1,34	1,43	1,24	[a]C
	Z	8,00	8,00	8,00	8,00	8,00	8,00	
	Al (VI)	1,50	1,37	1,30	1,47	1,67	1,57	(Mean=356.2 ºC;
	Cr	0,01	0,00	0,00	0,00	0,00	0,00	Std. Dev. =
	Fe	8,21	8,53	8,36	8,32	8,33	8,16	26.1 ºC)
	Ni	0,00	0,00	0,00	0,00	0,00	0,00	
	Mg	2,07	1,97	2,19	2,04	1,77	2,01	
	Mn	0,03	0,03	0,02	0,04	0,06	0,02	
	Ti	0,00	0,00	0,00	0,00	0,00	0,00	
	Y	11,82	11,89	11,88	11,88	11,83	11,77	
	Ca	0,03	0,04	0,05	0,03	0,03	0,04	
	Na	0,05	0,01	0,03	0,02	0,03	0,03	
	K	0,02	0,02	0,02	0,02	0,00	0,01	
	X	0,10	0,07	0,10	0,07	0,07	0,08	
	XYZ	19,92	19,96	19,97	19,95	19,89	19,85	
	XFe	0,80	0,81	0,79	0,80	0,82	0,80	
Garnet – Biotite (**)		6-16 Bt	6-16 Grt	6-18 Bt	6-18 Grt	6-21 Bt	6-21 Grt	
	SiO_2	32,37	36,04	31,65	35,62	33,07	35,94	
	TiO_2	1,88	0,00	1,83	0,03	1,68	0,01	573.6
	Al_2O_3	15,16	20,35	15,18	20,20	14,90	20,08	to
	Cr_2O_3	0,04	0,04	0,03	0,01	0,02	0,02	591.2 ºC
	FeO	26,52	34,31	29,58	35,48	25,65	34,89	(Mean=583.8 ºC;
	MnO	0,17	2,17	0,17	2,10	0,17	2,31	Std. Dev. =
	MgO	4,83	1,18	5,35	1,16	5,21	1,35	9.2 ºC)
	CaO	0,00	3,62	0,11	3,59	0,00	3,86	
	Na_2O	0,05	0,00	0,09	0,00	0,04	0,00	
	K_2O	8,89	0,01	8,04	0,01	8,12	0,01	
	Total	89,90	97,72	92,01	98,21	88,86	98,47	

The close grouping of the obtained $\delta^{34}S$ values (Table 5) indicates that the sulphur very likely originated from the same source. The difference between the different minerals (Table 5) may reflect the isotopic equilibration among minerals and between the minerals and mineralizing fluids. It should also be taken into account that for most of the samples a pure sulphide concentrate was not obtained and, hence, the contamination of each sample with various sulphide phases will cause shifts in the $\delta^{34}S$ values.

Table 5. Sample descriptions and results obtained for the S-isotope investigation. The values in brackets represent the standard deviation of the $\delta^{34}S$ values

Sample	Description	$\delta^{34}S$ value
SP2-1	Mosteiros: Euhedral pyrite in carbonatized tuff (possible contamination with tetrahedrite, ilmenite and chalcopyrite)	-3.0‰ (0.031)
96-2-4	São Martinho: Pyrite II veinlet	-3.8‰ (0.020)
96-2-1	São Martinho: Pyrrhotite (possible contamination with chalcopyrite)	-6.5‰ (0.033)
96-1-7	São Martinho: Anhedral arsenopyrite II and pyrrhotite (intergrown) – RSII stage	-4.7‰ (0.025)
96-1-7A	São Martinho: Anhedral arsenopyrite II and pyrrhotite (intergrown) – RSII stage	-5.3‰ (0.024)
96-1-13	São Martinho: Disseminated arsenopyrite and pyrrhotite in banded amphibolite – RSI stage	-4.9‰ (0.019)

However, at São Martinho there is a late episode of magmatically influenced mineralization and, hence, it is likely that this event should show magmatic sulphides with characteristic $\delta^{34}S$ values close to zero. However, Table 5 indicates that the sulphides from São Martinho show $\delta^{34}S$ values between -3.8 and -6.5 ‰. A late magmatic episode of mineralization is not recognized at Mosteiros. Nevertheless, $\delta^{34}S$ values of -3.0 ‰ have been obtained. Therefore, it is postulated that the shift towards more negative $\delta^{34}S$ values are indicative of the interaction between the ore-forming hydrothermal fluids and the host wall rocks (Série Negra metasedimentary rocks).

GENERAL DISCUSSION

Preamble

Several analogies between orogenic lode-gold deposits, be they Archaean lode-gold deposits or Phanerozoic lode-gold deposits as defined by Hagemann and Cassidy (2000) and Bierlein and Crowe (2000), respectively, can be drawn with features highlighted in this study of the São Martinho and Mosteiros areas. Hence, these prospects can be classed as orogenic lode-gold type. Analogies between orogenic lode-gold deposits and the São Martinho and Mosteiros prospects exist in: (1) collisional geotectonic controls; (2) metamorphism (grade and sense of P-T paths); (3) structural controls on mineralization; (4) ore mineral assemblage and chemistry; (5) mineralization and source of mineralizing fluids; (6) $\delta^{34}S$ values; (7) wall-rock alteration; and (8) timing of mineralization.

Local analogies with other worldwide orogenic lode-gold deposits

(Collisional) geotectonic controls - Although a corridor of blastomylonitic rocks separates the São Martinho and Mosteiros areas, these prospects are well constrained within the Tomar

Cordoba Shear Zone. This shear zone appears to be the result of highly oblique convergent processes of continental collision (Gumiel and Campos, 2001) throughout the evolution of the Iberian Massif as a result of the Variscan Orogeny.

There is no doubt that western Europe is the result of the amalgamation of several terranes brought together by collisional tectonics and continental growth processes throughout the Palaeozoic. Presently, these terranes are separated from one another by discrete faults (Shelley and Bossière, 2000). These types of accretionary/collisional settings are indicated as prime sites for the development of orogenic lode-gold mineralization.

The European Variscides, extending from the Iberian Peninsula to Bohemia, are the result of continental collision between Gondwana and Baltica from which resulted the Variscan polyphase orogeny. This lasted more than 100 Ma (Bouchot *et al.*, 2000) from the Late Devonian to the late Carboniferous, although in a broader sense it includes events of Early Devonian and Late Silurian age (Eguíluz *et al.*, 2000). This orogeny comprises three successive periods - Eovariscan, Mesovariscan and Neovariscan. The Eovariscan (450-400 Ma) is characterized by the burial of oceanic and continental units during resorption of the Early Palaeozoic ocean by subduction. The Mesovariscan (400-350 Ma) is characterized by major thrusting events responsible for crustal thickening in the internal zone of the orogen and ends by early exhumation and lithospheric detachment. The Neovariscan (325-290 Ma) is marked by progressive transition from a compressional to a generalized extensional regime characterized by major normal faults, return to equilibrium of the thickened crust, widespread granite intrusion and granulitization of the base of the crust probably related to subcrustal accretion of basic magma at about 300 ± 15 Ma (Bouchot *et al.*, 2000). As to the probable age of the TCSZ, there are currently two schools of thought: (1) a Variscan age; and (2) a continuous tectonometamorphic process from the latest Proterozoic (Cadomian?) to the latest Palaeozoic (J. B. Silva, 2004, pers. commm.).

Metamorphism - Structurally hosted lode-gold deposits of all ages, from Archaean to the present, are found in metamorphic terranes (Nesbitt, 1991; Kerrich, 1993) and this is perhaps the one unifying feature and fundamental constraint of this deposit type. A determining factor in lode-gold deposits is that they are typically found within rocks that range in metamorphic grade from subgreenschist to amphibolite facies (Colvine, 1989; Bierlein and Crowe, 2000) similarly to what happens within the study area (i.e. the Mosteiros mineralization is hosted in greenschist grade rocks while at São Martinho the rocks reach amphibolite grade). Generally, the metamorphic history of these rocks hosting orogenic lode-gold deposits also reflect a clockwise P-T(-t) path (Bickle *et al.*, 1985; Dalstra *et al.*, 1997; Ridley *et al.*, 1997), which is also analogous with that of the Série Negra rocks within the Iberian Peninsula (e.g. Abalos *et al.*, 1991b; Abalos Vilaro, 1992; Ordoñes-Casado, 1998).

Structural controls for mineralization - The strong structural control of lode-gold mineralization is evident on a variety of scales. In summary, Bierlein and Crowe (2000) and Hagemann and Cassidy (2000) exemplify four general structural styles important to trapping mineralization : (1) breccias associated with high-angle to low-angle reverse strike-slip faults; (2) stockwork networks, vein sets, and extensional fracture arrays in competent rocks; (3) laminated veins in shear zones and fold hinges in ductile turbidites; and (4) predominantly ductile shear zones, hosting thin, discontinuous, highly attenuated and deformed veins. Also, the structural framework of deposits within, or adjacent to granites and within high-grade basement rocks is commonly defined by multiple intersecting sets or by an anastomosing network of subvertical shear zones, with ore shoots located at the intersections between first-order and second-order shears (Boyle, 1990; Hodgson, 1993a; Marignac and Cuney, 1999).

The lack of sufficient exposure of the structures that host mineralization and the advanced state of weathering of the host rocks, as well as the lack of underground works at São Martinho and Mosteiros precludes the precise recognition of the structural controls for gold mineralization. However, the presence of mineralized breccias at Mosteiros and the quartz vein systems recognized in the São Martinho core are analogous to mineralization styles observed in several other lode-gold deposits.

Ore mineral assemblage and ore mineral chemistry - The vast majority of lode-gold deposits, in (Phanerozoic) orogenic belts, are characterized by very consistent vein mineralogies and parageneses (Bierlein and Crowe, 2000). The mineralogy of these deposits is simple and essentially comprises quartz (70-95 % of total vein volume) with Fe-Mg ± Ca carbonates, alkali feldspar, sericite, chlorite, sulphides and gold (Boyle, 1986). The ore and gangue minerals observed at São Martinho and Mosteiros are consistent with those found in other lode-gold deposits. However, many other deposit types would also comprise these sorts of minerals.

Native gold is consistently pure (> 90%) and silver contents generally remain below 2-5 wt % in most lode-gold occurrences (Bierlein and Crowe, 2000). However, Goldfarb *et al.* (1989), reported silver contents of between 13 and 50 wt % in the Juneau gold belt and So and Yun (1997) reported silver contents of between 4 and 25 wt % in granite-hosted lode-gold deposits in central Korea. Native gold at Mosteiros is very pure ($Au_{98.6}$), whereas gold at São Martinho shows slightly different compositions. Gold I (RS I "lode gold") is $Au_{88.35}$ with $Ag_{7..62}$ while gold II (RS II - "overprint gold") is $Au_{84.12}$ and Ag_{15}. Considering that gold II is not regarded as orogenic lode gold, the variations observed as well as the chemistry of the gold grains are consistent with published data.

Source of mineralising fluids - Mineralising fluids in lode-gold deposits are generally agreed to have formed at relatively deep levels within the crust during active tectonism (Ridley and Diamond, 2000). Although there is no conclusive evidence for the origin of the fluids, the main models proposed for the generation of gold-transporting hydrothermal fluid of lode-gold deposits include:

(1) metamorphic devolatilization during prograde, regional metamorphism of greenstone belts, proposed by Kerrich and Fyfe (1981), Phillips and Groves, (1983), Powell *et al.* (1991) and Murphy and Roberts (1997) as a possible source of the mineralizing fluid. The fluid is considered to be released from hydrous (and carbonate) minerals on their breakdown in prograde metamorphic reactions. Since shear zones and other structures consist of too small a volume of altered rock to supply the amount of gold in lode-gold deposits, Ridley and Diamond (2000) proposed that the gold was leached from dehydrating rocks or from nearby rocks along the flow path before the fluid was channelled. Furthermore, Powell *et al.* (1991) and Phillips and Powell (1993) proposed that the fluid is released from rocks with a significant mafic component (e.g. greywackes), at the greenschist to amphibolite transition;

(2) devolatilization of the lower and/or middle crust with or without input from the mantle has been proposed as a possible source for the mineralizing fluids (e.g. Cameron, 1988; Colvine, 1989; Fyon *et al.*, 1989);

(3) the devolatilization of felsic magmas [extensive regional batholiths and/or specific granitic associations (Mueller, *et al.*, 1991)]. The fluid is considered to have been exsolved from crystallizing granitic magmas (second boiling). Gold, being an incompatible element during crystallization, would be concentrated in the magmatic fluid and the changing fluid-rock equilibrium with cooling or with infiltration of country rock are viewed as the driving forces for gold deposition (Ridley and Diamond, 2000). Felsic rock types that

have been proposed for the fluid source include tonalite-trondhjemite-granodiorite magmas (Burrows and Spooner, 1987; 1989), oxidized alkaline suites (Cameron and Hattori, 1987) and evolved granitic sources (Ramsay *et al.*, 1998; Qiu and McNaughton, 1999). However, there is yet no evidence as to which granite types produce the fluids with the correct composition such as those found in lode-gold deposits (Ridley and Diamond, 2000);

(4) fluid release during crystallization of gold-rich shoshonitic-lamprophyre magmas (Rock *et al.*, 1989) or their interaction with crustal rocks (Ridley and Diamond, 2000) is also viewed as a possible source of ore fluids; and

(5) meteoric waters that have infiltrated and circulated to great depths in the crust (Nesbitt, 1988; Nesbitt and Muellenbachs, 1991).

Evidence from the fluid inclusions study in the area suggests that the source of the mineralizing fluids within the São Martinho area is thought to be firstly, a mixture of dilute brines (H_2O-NaCl) containing CO_2 and CH_4 derived from metamorphic devolatilization reactions, e.g. dehydration reactions in pelites of the Série Negra (e.g. Azuaga and Atalaya Formations, Spain) of the type: chlorite + K-spar = biotite + chlorite + quartz + H_2O have been documented on the Spanish side of the TCSZ by Abalos Vilaro (1992, p. 162), and the emplacement of syntectonic (Variscan) granitoid bodies (e.g. Mte. Aguilhão, Bedanais and Mte. Barquete granitoids; Fig.1) and, secondly, a later, hotter, hypersaline fluid derived from the emplacement of late-post Variscan felsic magmas. These features are consistent with those occurring in other well-known lode-gold deposits.

Fluid trapping temperatures for several lode-gold deposits are indicated to occur anywhere between 140 and 450 ºC. Local variation within deposits can be large (e.g. Annels and Roberts, 1989; Kontak *et al.*, 1990; Goldfarb *et al.*, 1993; Gao and Kwak, 1995a, b; Ashley and Craw, 1995; So and Yun, 1997; Ryan and Smith, 1998; Mernagh, 2001) and the trapping temperatures of the fluids (Table 3), measured at São Martinho are well within this range.

Sulphur isotopes - Sulphur isotope compositions of sulphides in some worldwide lode-gold deposits range from 0 to 9‰ $\delta^{34}S$ (Kerrich, 1987; Golding *et al.*, 1990), which indicates that the sulphur source was isotopically uniform and derived directly from the mantle, from magmas, or indirectly by dissolution and/or desulphidation of primary sulphide minerals or average crustal sulphur (Hagemann and Cassidy, 2000). However, other studies (e.g. Hagemann *et al.* 1999) report that mineralization controlled by major brittle-ductile zones (Fimiston-style) and mineralization characterized by major breccia ore bodies (Oroya-style) lodes, typical of the Golden Mile deposit located in the Kalgoorlie terrane of the Yilgarn Craton of Western Australia (Hagemann and Cassidy, 2000), have far greater ranges in $\delta^{34}S$ values from -10 to +18‰. In the Meguma terrane (Nova Scotia, Canada), $\delta^{34}S$ values, both proximal and distal to intrusions, vary from 10 to 30‰, which suggests that appreciable amounts of sulphur could have been derived from biogenic and inorganic reduction of sulphate in the host sediments (Sangster, 1992; Kontak and Smith, 1993). Also, gold deposits in Victoria (Lachlan Fold Belt) have $\delta^{34}S$ that range from -3 to +8‰ for base metals, while pyrite values hover around 15‰ (Green *et al.*, 1982). Palin and Xu (2000) indicated $\delta^{34}S$ values in pyrite from the Victory mesothermal gold deposit (south of Kambalda, Yilgarn Craton, Australia) ranging from -4.4 to +5.1‰. Alternatively, Hodgson (1993b) indicated that the $\delta^{34}S$ values obtained in Phanerozoic lode-gold deposits cluster around 0‰ and point to the derivation of the sulphur from a magmatic source or dissolution of primary magmatic sulphide minerals by hydrothermal fluids.

Isotope compositions of S for lode-gold deposits vary greatly and are probably inconclusive as a distinguishing feature in this type of deposit. At São Martinho and Mosteiros the $\delta^{34}S$ values obtained cluster closely with negative values indicating either a possible similar magmatic source for the sulphides or the interaction between the mineralizing hydrothermal fluids and the host rocks.

Wallrock alteration - In terms of wallrock alteration, typical lode-gold deposit-type alteration assemblages are observed at São Martinho and Mosteiros, i.e. silicification, carbonatization, sericitization, chloritization ± tourmalinization and subdued albitization.

Timing of mineralization - The timing of mineralization is not well constrained at São Martinho and Mosteiros due to the lack of geochronological data. However, as in other lode-gold deposits, the peak of mineralization is inferred to have occurred after, but close to peak metamorphism. Subsequent overprinting of this stage of mineralization occurs with the emplacement of late-post-Variscan granite magmas. Several lode-gold deposits throughout the world have also suffered overprints by subsequent mineralizing events.

TOWARDS AN ORE GENESIS MODEL FOR THE SÃO MARTINHO AND MOSTEIROS PROSPECTS

Introduction

A generic ore genesis model is presented that encompasses the characteristics of both the Mosteiros and São Martinho prospects. However, the model is heavily biased by the greater amount of data available from the São Martinho prospect and is based on the available mineralogical, structural and geochronological data.

Ore genesis model

The maximum age of deposition of the Série Negra (Tentúdia Group) in Spain has been interpreted to be *c.* 550 Ma (Schäfer *et al.*, 1993). Hence, the mineralization hosted within the Série Negra metasedimentary rocks will post-date 550 Ma.

Peak metamorphism is interpreted to have occurred at ~345-335 Ma Ordoñes-Casado (1998). The processes responsible for initial ore formation (lode-gold stage; RS I) are inferred to have taken place in the latter stages of peak metamorphism and possibly slightly beyond peak metamorphic conditions (Fig. 5). All tectonothermal events leading to peak metamorphism are believed to have taken place under a compressional regime *(s.l.)* that is interpreted from the textural relationships observed in the ore minerals and their association with gangue minerals. QI veinlets from São Martinho immediately followed metamorphism. Notwithstanding the fact that primary fluid inclusions are absent from QI veinlets, the secondary fluid inclusion population are mostly parallel to mineralized fractures thereby indicating that the secondary fluid inclusions most probably represent the primary mineralizing fluids.

Metamorphic devolatilization reactions occurring in the pelitic component of the Série Negra metasedimentary rocks supplied the fluids responsible for ore formation and the driving force for fluid migration. There is no precise geochronological data that indisputably corroborates this fact, but this can be inferred given the overwhelming similarities of the mineralization style in the study area with orogenic lode-gold deposits elsewhere. These fluids would have

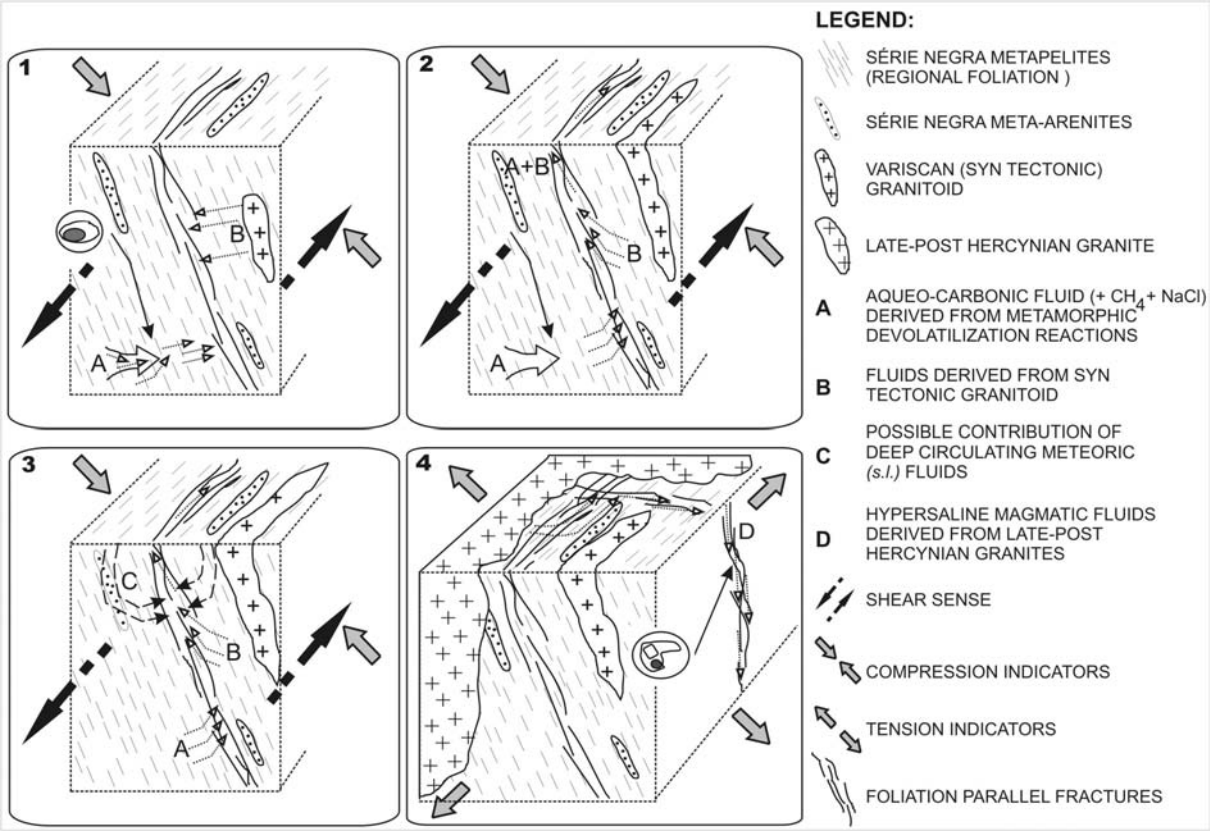

Figure 10: *Schematic ore genesis model for the São Martinho area. 1- derivation of fluids from metamorphic devolatilisation reactions (A) in pelites of the Série Negra and possible contribution by syntectonic granitoids (B) (if coeval with mineralization); leaching of metals from metasedimentary rocks, 2- channeling of fluids along incipient fractures parallel to the regional foliation, emplacement of lode-gold type mineralization (RS I), 3- Possible contribution of surface/meteoric waters, 4- emplacement of late- to post-tectonic granites, release of hypersaline, magmatic fluids and focusing of the same fluids along cross-cutting wrench faults/fractures; precipitation of high-temperature sulphide assemblage and gold II (RS II). Note: Diagram is not to scale; each successive stage takes place at a higher stratigraphic level due to continuous uplift; all surfaces represented by dashed lines (apart from arrows) are slices through the Série Negra at depth. North is to the right in all images.*

been concentrated along incipient fractures parallel to regional foliation (WNW-ESE) (Fig. 10-1). In addition, the syntectonic granite bodies (Aguilhão, Bedanais, Barquete) also provided the thermal energy and possibly, if they were coeval with the regional metamorphic fluids, fluids that would mix and be channelled in faults/fractures (Fig. 10-1).

The early, moderate temperature and salinity (although variable), H_2O-CO_2-NaCl (+CH_4) fluids (Fig. 10-2), responsible for the early paragenesis (RS I) of São Martinho ore minerals while Variscan tectonism *(s.l.)* was still active, would have leached metals from the Série Negra sediments. The early paragenesis, consisting primarily of pyrite I and II, chalcopyrite I and I', pyrrhotite I, arsenopyrite I and gold I, was deposited in early-stage fractures around the time following metamorphism (i.e. immediately after 345-335 Ma). The ore mineral textures show that this early ore mineral paragenesis was trapped in the host rocks while tectonism was active (e.g. arsenopyrite I pods are stretched parallel to regional foliation). Fluid inclusions indicate that at São Martinho trapping pressures of fluid inclusions would have been ~4-7 kbar. The fluid inclusion data shows that fluid modification processes may have taken place resulting in an immiscible phase of this early fluid (i.e. an H_2O-NaCl and a H_2O-

$NaCl\text{-}CO_2$ fluid). Phase separation is indicated as a probable agent for precipitating ore minerals in lode-gold deposits (Hagemann and Cassidy, 2000). The fact that the fluids contain CH_4 further substantiates their evolution and migration through the carbon-rich Série Negra. Since the geochemistry of the Série Negra rocks also corroborates the presence of an ancient arc-like setting, as proposed by Pereira and Silva (2001), circulating meteoric and saline waters are probable and could mix with the ore mineralizing fluids (De Oliveira, 2001a; Fig. 10-3).

In São Martinho, this early phase of mineralization is accompanied by discrete quartz, chlorite, muscovite-sericite, tourmaline (fine) and albite alteration assemblages around pyrite I veinlets. Some alteration assemblages are subdued and difficult to distinguish as discussed previously. Conversely, at Mosteiros there is a pervasive ferroan dolomite alteration that all but obliterates any other alteration minerals associated with ore mineralization. The materials at Mosteiros did not lend themselves to obtaining microthermometric fluid inclusion data and hence there is no way to tell if the ore mineral paragenesis observed at Mosteiros was derived from a similar fluid to the one at São Martinho. The partial, limited similarity in wallrock alteration assemblages in the two areas might argue favourably for this.

At São Martinho there is a clear overprinting of the early phase of mineralization (RS I) with a later, higher temperature, mineralizing event (RS II). This second event is characterized by higher temperature ore minerals (loellingite) as well as pyrite III, chalcopyrite II, pyrrhotite II, arsenopyrite II and a second generation of gold (gold II). The overprinting event is associated with quartz II (QII) veins that contain hypersaline fluid inclusions (Fig. 10-4). These fluid inclusions often show homogenization temperatures in excess of 550 ºC. Their morphology and very high homogenization temperatures would indicate a probable magmatic origin for these fluids (i.e. derived from late- to post-Variscan granitoid magmas, Fig. 10-4).

This event (RS II) is probably linked to late Variscan wrench faults and fractures that are orientated N-S and cross-cut the regional foliation. In shallow trenches opened at São Martinho (Camm, 1996) it was noted that several small (<0.50m-thick) quartz veins were aligned parallel to regional N-S wrench faults and showed evidence of sulphide mineralization. Gonçalves *et al.* (1978) postulated that the opening of these fractures occurred in Upper Westphalian times (~305 Ma). This period is coincidental with metalliferous peaks for orogenic (Au, Sb, W) deposits that occurred at around 310-305 Ma within the Variscan Belt of western Europe (Bouchot *et al.*, 2000). This interval is linked to a Neovariscan hydrothermal event that generates epigenetic, post-metamorphic and structurally controlled deposits. The effect of dilation between rigid blocks separated by these late-Variscan fractures was to create open spaces (Gumiel and Campos, 2001) that are now quartz-filled and cross cut the regional foliation of the Série Negra rocks. These quartz veins are quartz II (QII) veins that host visible gold (II) mineralization. Following this line of reasoning, the RS I event (early lode-gold stage) in São Martinho would be older than 305 Ma and would be related to the period just after peak metamorphic conditions (i.e. <345-335 Ma). Hence, the RS II event (late remobilization stage) in São Martinho would have taken place in the period where the crust was under tension *(s.l.)* while fractures were opening up, i.e. < 305 Ma (Lower Permian upwards) (De Oliveira, 2001a, b).

In summary, the genesis of the mineralization can be explained in terms of cross-cutting relationships between QI and QII veins whereby the area passed from a regime of compression to one of tension *(s.l.)* in the late stages of the Variscan Orogeny. During a state of compression, a typical orogenic lode-gold style mineralization was generated while during

a state of tension *(s.l.)* the initially formed mineralization (RS I) was remobilised by hotter and more saline fluids creating the RS II paragenesis in São Martinho.

The single borehole studied in Mosteiros does not show evidence of such discrete quartz veining as the São Martinho boreholes do. The core is characterized by a much more subdued silicification event and quartz veining cross-cutting relationships with the host Série Negra rocks and mineralization are not clear. In Mosteiros there is no recognition of two separate mineralizing events and hence, also the recognition of mineralizing events related with syn-Variscan or post-Variscan structures. The low gold grades obtained here result from gold trapped within the lattices of the host sulphide minerals and the few small gold grains observed in the samples. These gold grains were not detected in sufficient number to allow the definition of a consistent paragenetic sequence in relation to the host sulphide minerals and hence, any predictions remain speculative at this stage. However, gold mineralization at Mosteiros seems to be related to a single mineralizing event associated with pervasive ferroan dolomite alteration and brecciation stages that are not constrained, either geochronologically, or in terms of accurate age of their sequential minerals. This one event is limitedly, vaguely similar to the RS I event at São Martinho and hence possibly interpreted to have occurred at hypothetical peak and post-peak metamorphic conditions.

ACKNOWLEDGEMENTS

This study represents in large the research for a Doctor of Philosophy (Ph.D) degree in Science undertaken at the *Economic Geology Research Institute-Hugh Allsopp Laboratory* (EGRI-HAL), *University of the Witwatersrand* (Republic of South Africa) by the senior author and supervised by the co-authors. This work also results from a protocol of collaboration entered into by the *Instituto Geológico e Mineiro* (Portugal) and the *University of the Witwatersrand.* DPSdeO would like to acknowledge the valuable contribution of Prof. F. Roland Merkle and Mr. Peter Grasse of the University of Pretoria in supplying microprobe facilities. DPSdeO benefited from a *Praxis XXI PhD bursary (BD/15877/98)* awarded by the *Fundação para a Ciência e a Tecnologia*. Messrs. A. Gouveia, A. Verde and A. Mathebula are thanked for polished thin section preparation. Mr. J. L. Pinto is thanked for help with sample collection and general field work.

REFERENCES

Abalos Vilaro, B., 1992. Cinematica y mecanismos de la deformacion en regimen de transpresion. Evolucion estrutural y metamorfica de la zona de cizalla ductil de Badajoz Cordoba. Serie NOVA TERRA, Nº6. Edicios do Castro, 430p.

Abalos, B. and Eguiluz, L., 1992a. Evolución geodinámica de la zona de cisalla dúctil de Badajoz-Córdoba durante el Proterozoico Superior-Câmbrico Inferior. In: Paleozoico Inferior de Ibero-América, Gutiérrez-Marco, J.C.; Saavedra, J. & Rábano, I., (eds.), Universidad de Extremadura, 577-591.

Abalos, B. and Eguiluz, L., 1992b. The late Proterozoic suture zone of SW Iberia: a link for the reconstruction of the Cadomian-Avalonian-Panafrican transpressive orogen of the Circum-Atlantic region. Comptes Rendus de l'Académie des Sciences, t. 314, Série II, p. 691-698.

Abalos, B., Gil Ibarguchi, J.I., and Eguiluz, L., 1991a. Cadomian subduction/collision and Variscan transpression in the Badajoz-Córdoba Shear Belt. (SW Spain). Tectonophysics, 199, 51-72.

Abalos, B., Eguiluz, L., and Gil Ibarguchi, J. y J.I., 1991b. Evolución tectono-metamórfica del Corredor Blastomilonítico de Badajoz-Córdoba. II. Las unidades alóctonas y

trajectorias PTt. Boletín Geológico y Minero, 102-5, 617-671.
Annels, A.E. and Roberts, D.E., 1989. Turbidite-hosted gold mineralization at the Dolaucothi gold mines, Dyfed, Wales, United Kingdom. Economic Geology, 84, 1293-1314.
Ashley, P.M. and Craw, D., 1995. Carrick Range Au and Sb mineralization in Caples terrane. Otago Schist, central Otago, New Zealand. New Zealand Journal of Geology and Geophysics, 38, 137-149.
Ashley, P.M., Creagh, C.J. and Ryan, C.G., 2000. Invisible gold in ore mineral concentrates from the Hillgrove gold-antimony deposits, NSW, Australia. Mineralium Deposita, 35, 285-301.
Azor, A., Gonzaléz Lodeiro, F. and Simancas, J.F., 1994. Tectonic evolution of the boundary between the Central Iberian and Ossa Morena Zones (Variscan Belt, southwest Spain). Tectonics, 13, 45-61.
Berthé, D, Choukroune, P and Jegouzo, P., 1979. Orthogneiss, mylonite and non coaxial deformation granites: the example of the south Armorican shear zone. Journal of Structural Geology, 1, 31-42.
Bickle, M.J., Morant, P., Bettenay, L.F., Boulter, A.C., Blake, T.S. and Groves, D.I., 1985. Archean tectonics of the Shaw Batholith, Pilbara Block Western Australia: Structural and metamorphic tests of the batholith concept. Geological Association of Canada Special Paper, 28, 325-341.
Bierlein, F.P. and Crowe, D.E., 2000. Phanerozoic orogenic lode gold deposits. In: Hagemann, S.G. and Brown, P.E. (eds.), Gold in 2000. Reviews in Economic Geology, 13, 103-139.
Blatrix, P. and Burg, J.P., 1981. ^{40}Ar-^{39}Ar dates from Sierra Morena (Southern Spain): Variscan metamorphism and Cadomian orogeny. Neues Jahrbuch Mineralogie Monatshefte, 1981/10, 470-478.
Bohlen, S.R., 1987. Pressure-temperature-time paths and a tectonic model for the evolution of granulites. Journal of Geology, 95, 617-632.
Bouchot, V., Milesi, J.P. and Ledru, P., 2000. Crustal-scale hydrothermal palaeofield and related Variscan Au, Sb, W orogenic deposits at 310-305 Ma (French Massif Central, Variscan Belt). Society for Geology Applied to Mineral Deposits (SGA) News, Dec. 2000, Nº 10, p.1, 6-12.
Boyle. R.W., 1986. Gold deposits in turbidite sequences: Their geology, geochemistry and history of the theories of their origin. Geological Association Canada Special Paper 32, 1-13.
Boyle, G.O., 1990. Hillgrove antimony-gold deposits: Australian Institute of Mining and Metallurgy Monograph 15, I, 1425-1427.
Burg, J.P., Iglesias, M., Laurent, P.H., Matte, P. and Ribeiro, A., 1981. Variscan intracontinental deformation: The Coimbra-Córdoba Shear Zone (SW Iberian Peninsula). Tectonophysics 78, 161-177.
Burrows, D.R. and Spooner, E.T.C., 1987. Generation of a magmatic H_2O-CO_2 fluid enriched in Mo, Au and W within an Archean sodic granodiorite stock, Mink Lake, northwestern Ontario. Economic Geology, 82, 1931-1957.
Burrows DR, Spooner ETC (1989) Relationship between Archean gold-quartz vein-shear zone mineralization and igneous intrusions in the Val d'Or and Timmins areas, Abitibi Subprovince, Canada. In: Keays RR, Ramsay WRH, Groves DI (eds) The Geology of Ore Deposits: The perspective in 1988, Economic Geology Monograph 6: 424-444.
Cameron, E.M., 1988. Archean gold: relation to granulite formation and redox zoning in the crust. Geology, 16, 109-112.
Cameron, E.M. and Hattori, K., 1987. Archean gold mineralization and oxidised hydrothermal fluids. Economic Geology, 82, 1177-1191.
Carrilho Lopes, J. M., Lisboa, J. L. and Lisboa, J. V., 1997. Caracterização petrográfica e

estrutural dos granitos róseos do Complexo Plutónico de Monforte-Stª Eulália (NE Alentejo, Portugal). Estudos, Notas e Trabalhos do IGM, t. 39, 141-156.

Cathelineau, M., 1988. Cation site occupancy in chlorites and illites as a function of temperature. Clay Minerals, 23, 471-485.

Clark, L. A., 1960. The Fe-As-S system: Phase relations and applications-part II. Economic Geology, 55, 1631-1652.

Colvine, A.C., 1989. An empirical model for the formation of Archean gold deposits: products of final cratonization of the Superior Province, Canada. In: Keays, R.R., Ramsay, W.R.H. and Groves, D.I. (eds.), The Geology of Ore Deposits: The perspective in 1988, Economic Geology Monograph 6, 37-53.

Dalstra, H.J., Bloem, E.J.M. and Ridley, J.R., 1997. Gold in amphibolite facies terrains and its relationship to metamorphism, exemplified by the syn-peak metamorphic gold in the Transvaal deposit, Yilgarn Block, Western Australia. Chronique de la Reserche Minière, 529, 3-24.

De Oliveira, D.P.S., 1998. The rare earth-bearing Llandeilian quartzites in the Vale de Cavalos-Portalegre area, Central Iberian Zone, Portugal - Their better understanding through geological mapping and rock geochemistry. Comunicações, Actas do V Congresso Nacional de Geologia, t84, Fasc. 1, B142-B145.

De Oliveira, D.P.S., 2001a. The nature and origin of gold mineralization in the Tomar Cordoba Shear Zone, east central Portugal. Ph.D. Thesis, University of the Witwatersrand (Unpubl.), 352p.

De Oliveira, D.P.S., 2001b. Primary lode gold mineralization vs. magmatically remobilised gold mineralization at São Martinho (Tomar Cordoba Shear Zone): Its timing deduced from structural relationships. In: Livro das Apresentações Científicas e Livro-Guia de Excursão, 7ª Conferência Anual do Grupo de Geologia Estrutural e Tectónica (GGET2001), 51-54.

De Oliveira, D.P.S. 2003. The Mosteiros orogenic lode gold prospect, east-central Portugal: a case study for the occurrence of invisible gold. In: Eliopoulos *et al.*, (eds.), SGA 7 - Proceedings of the Seventh Biennial SGA Meeting on Mineral Exploration and Sustainable Development, Athens, Greece, August 24-28, 2003; Millpress (Rotterdam), p.755-758.

De Oliveira, D.P.S., Robb, L.J. and Inverno, C.M.C., 2001a. The São Martinho gold occurrence, NE Ossa Morena Zone, Portugal: Geological setting and ore genesis. In: Piestrzynski *et al.*, (eds.), Mineral Deposits at the Beginning of the 21st Century, Proceedings of the Joint Sixth Biennial SGA-SEG Meeting/Kraków, Poland/26-29 August 2001, 791-793.

De Oliveira, D.P.S., Shepherd, T., Naden, J. and Yao, Y., 2001b. Evidence for a late magmatic gold remobilising event in a mesothermal temperature setting at São Martinho, NE Ossa Morena Zone, Portugal. In: Noronha, F., Dória, A. and Guedes, A. (eds.). ECROFI XVI European Current Research On Fluid Inclusions - Abstracts, Universidade do Porto, Fac. De Ciências, Depto. de Geologia. Memórias nº7, 349-351.

De Oliveira, D.P.S., Poujol, M. and Robb, L.J., 2002a. U-Pb geochronology for the Barreiros tectonised granitoids and Arronches migmatitic gneisses: Tomar Cordoba Shear Zone, east central Portugal. Revista Sociedad Geológica España 15 (1-2): 105-112.

De Oliveira, D.P.S., Yao, Y. and Robb, LJ, 2002b. Remobilization of gold mineralization in the São Martinho prospect, Tomar Cordoba Shear Zone (TCSZ), east central Portugal: Constraints from fluid inclusions. Economic Geology Research Institute-Hugh Allsopp Laboratory (EGRI-HAL) Information circular, 364, 15p.

De Oliveira, DPS, Reed, RM, Milliken, KL, Robb, LJ, Inverno, CMC and d'Orey, FLC, 2003a. (Meta)cherts, (meta) lyddites, (meta)phthanites and quartzites of the Série Negra (Crato-São Martinho), E. Portugal: towards a correct nomenclature based on

mineralogy and cathodoluminescence studies. Ciências da terra (UNL), Lisboa, nº especial V, CD_ROM, B68-B71.

De Oliveira, DPS, Reed, RM, Milliken, KL, Robb, LJ, Inverno, CMC and d'Orey, FLC, 2003b. Série Negra black quartzites – Tomar Cordoba Shear Zone, E Portugal: Mineralogy and cathodoluminescence studies. Cadernos do Laboratorio Xeolóxico deLaxe, 28, 193-211.

De Oliveira, DPS, Wiechowski, A, Robb, LJ, Inverno, CMC, 2003c. Amphibolite vs. Banded amphibolite: a case study in the São Martinho-Arronches area, Tomar Cordoba Shear Zone, NE Ossa Morena Zone, Portugal. Cadernos do Laboratorio Xeolóxico de Laxe, 28, 213-229.

Eguíluz, L., Ibarguichi, J.I.G., Ábalos, B. and Apraiz, A., 2000. Superposed Hercynian and Cadomian orogenic cycles in the Ossa Morena Zone and related areas of the Iberian Massif. GSA Bulletin, 112, 9, 1398-1413.

Ferry, J.M. and Spear, F.S., 1978. Experimental calibration of the partitioning of Fe and Mg between biotite and garnet. Contributions to Mineralogy and Petrology, 66, 113-117.

Fyon, J.A., Troop, D.G., Marmont, S. and Macdonald, A.J., 1989. Introduction of gold into Archean crust, Superior province, Ontario-Coupling between mantle-initiated magmatism and lower crustal thermal maturation. In: Keays, R.R., Ramsay, W.R.H. and Groves, D.I. (eds.), The Geology of Ore Deposits: The perspective in 1988, Economic Geology Monograph 6, 479-490.

Gao, Z.L. and Kwak., T.A.P., 1995a. Turbidite-hosted gold deposits in the Bendigo-Ballarat and Melbourne zones, Australia. I. Geology, mineralization, stable isotopes, and implications for exploration. International Geology Review, 37, 910-944.

Gao, Z.L. and Kwak., T.A.P., 1995b. Turbidite-hosted gold deposits in the Bendigo-Ballarat and Melbourne zones, Australia. II. Nature of ore fluids. International Geology Review, 37, 1007-1038.

Goldfarb, R.J., Leach, D.L., Rose, S.C. and Landis, G.P., 1989. Fluid inclusion geochemistry of gold-bearing quartz veins of the Juneau gold belt, southeastern Alaska: Implications for ore genesis. In: Keays, R.R., Ramsay, W.R.H. and Groves, D.I. (eds.), The Geology of Ore Deposits: The perspective in 1988, Economic Geology Monograph 6, 363-375.

Goldfarb, R.J., Snee, L.W. and Pickthorn, W.J., 1993. Orogenesis, high-temperature thermal events, and gold vein formation within metamorphic rocks of the Alskan Cordillera. Mineralogical Magazine, 57, 375-394.

Golding, S.D., Groves, D.I., McNaughton, N.J., Mikuchi, E.J. and Sang, J.H. 1990. Constraints on genesis of primary gold deposits. In: Ho, S.E., Groves, D.I. and Bennett, J.M. (eds.). Gold Deposits of the Archean Yilgarn Block, Western Australia: Nature, Genesis and Exploration Guides. Geology Department (Key Centre) and University Extension, University of Western Australia Publication nº20, 259-262.

Gonçalves, F, 1971. Subsídios para o conhecimento geológico do nordeste alentejano. Memória nº18 dos Serviços Geológicos de Portugal, 62p.

Gonçalves, F., and Fernandes, A. P., 1973. Notícia explicativa da folha 32-B (Portalegre). Serviços Geológicos de Portugal, 45p.

Gonçalves, F., Perdigão, J. C., Coelho, A. V. P. and Munhá, J. M., 1978. Notícia explicativa da folha 33-A (Assumar). Serviços Geológicos de Portugal, 37p.

Gonçalves, F., Carvalhosa, A., 1994. O Proterozóico da Zona de Ossa Morena no Alentejo. Síntese e actualização de conhecimentos. Memórias da Academia das Ciências de Lisboa, Tomo XXXIV, 3-35.

Green, A.H., Donnelly, T.H., Jahnke, F.M. and Keays, R.R., 1982. Evolution of gold-bearing veins in dykes of the Woods Point dyke swarm, Victoria. Mineralium Deposita, 17, 175-192.

Gumiel, P. and Campos, R., 2001. Implicaciones del modelo “dominó” de fallas tardihercínicas en el control y localización de las mineralizaciones auríferas deal área de La Codosera (rama noroeste de la Zona de Cizalla de Badajoz-Córdoba). Boletín Geológico y Minero, 112, 3, 103-112.

Hagemann, S.G. and Cassidy, K.F., 2000. Archean orogenic lode gold deposits. In: Hagemann, S.G. and Brown, P.E. (eds.), Gold in 2000. Reviews in Economic Geology, 13, 9-68.

Hagemann, S.G., Bateman, R. and Vielreicher, R., 1999. In situ sulphur isotope composition of pyrites from the Fimiston-and Oroya-style gold lodes in the Golden Mile Camp, Kalgoorlie: Implications for sulphur source(s) and depositional processes. Geological Society of America, Abstracts with Program, 31, nº 7, pA-32.

Hodgson, C.J., 1993a. Mesothermal lode-gold deposits. Geological Association of Canada Special Paper 40, 635-678.

Hodgson, C.J., 1993b. Mesothermal lode gold deposits. In: Kirkham, R.V., Sinclair, W.D., Thorpe, R.I. and Duke, J.M. (eds.) Mineral Deposit Modelling. Geological Association of Canada Special Paper 40, 635-678.

Inverno, C.M.C., 1995a. Relatório sobre seis sondagens para ouro da Sociedade Mineira Rio Artezia, Lda., (RIOFINEX) na região de Alter do Chão-Arronches (Portalegre). Faculdade de Ciências, Univ. de Lisboa (Internal Report), 26p.

Inverno, C.M.C., 1995b. Fuchsite and ferroan dolomite microprobe results from "mesothermal" gold mineralization at Mosteiros, Aronches, E. Portugal. Internal Report, Instituto Geológico e Mineiro, 8p.

Julivert, M., Fontboté, J.M., Ribeiro, A. and Conde, L., 1974. Mapa tectónico de la península Ibérica y Baleares, scale 1:1000000. Instituto Geológico y Minero España, 1-101.

Kerrich, R., 1987. The stable isotope geochemistry of Au-Ag vein deposits in metamorphic rocks. In: Kyser, T.K. (ed.) Mineralogical Association of Canada Short Course 13, 287-336.

Kerrich, R., 1993. Perspectives on genetic models for lode gold deposits. Mineralium Deposita, 28, 362-365.

Kerrich, R. and Fyfe, W.S., 1981. The gold-carbonate association: source of CO_2 and CO_2 fixation reactions in Archean lode gold deposits. Chemical Geology, 33, 265-294.

Kojonen, K. and Johanson, B., 1997. Ore microscopy and microprobe results of invisible gold in pyrite and arsenopyrite. In: Cabri, L.J., Criddle, A.J., Stanley, C.J., Vaughan, D.J. (technical organising committee), IMA/COM Short Course: Modern Approaches to Ore and Environmental Mineralogy, 8-10 September 1997, Laboratório do Instituto Geológico e Mineiro, S.Mamede de Infesta, Portugal, 18p.

Kontak, D.J. and Smith, P.K., 1993. A metaturbidite-hosted lode gold deposit. The Beaver Dam deposit, Nova Scotia. II Isotopic Studies. Economic Geology, 90, 885-901.

Kontak, D.J., Smith, P.K., Kerrich, R. and Williams, P.F., 1990. Integrated model for Meguma group lode gold deposits. Geology, 18, 238-242.

Kretschmar, U. and Scott, S.D., 1976. Phase relations involving arsenopyrite in the system Fe-As-S and their application. Canadian Mineralogist, 14, 364-386.

Kretz, R., 1983. Symbols for rock-forming minerals. American Mineralogist, 68, 277-279.

Marignac, C. and Cuney, M, 1999. Ore deposits of the French Massif Central: Insight into metallogenesis of the Variscan collision belt. Mineralium Deposita, 34, 472-504.

Mata, J. and Munhá, J., 1986a. Geochemistry of Cambrian metavolcanic rocks from the Córdoba-Elvas domain (Ossa Morena Zone). Maleo (Bol. Soc. Geol. Port.) 2 (13), 27.

Mata, J. and Munhá, J., 1986. Geodynamic significance of high-grade metamorphic rocks from Degolados-Campo Maior (Tomar Badajoz Cordoba Shear Zone). Maleo (Bol.

Soc. Geol. Port.) 2/13, 28.
Menéndez, L.G., 1998. Petrologia y geoquimica del batolito granitico de Nisa-Albuquerque (Alto Alentejo, Portugal, Extremadura, España). Ph.D. Thesis, Universidad de Granada (Unpubl.), 223p.
Mernagh, T.P., 2001. A fluid inclusion study of the Fosterville Mine: a turbidite-hosted gold field in the Western Lachlan Folf belt, Victoria, Australia. Chemical Geology, 173, 91-106.
Mueller, A.G., de Laeter, J.R., and Groves, D.I., 1991. Strontium isotope systematics of hydrothermal minerals from epigenetic Archaean gold deposits in the Yilgarn block, Western Australia. Economic Geology, 86, 780-809.
Moreira, A., 1994. Reconhecimento geológico, estrutural, petrográfico e geoquímico dos granitos de Alpalhão, Gáfete e Quarteleiros (Alto Alentejo). Estudos, Notas e Trabalhos, IGM, t.36: 103-117.
Murphy, P.J. and Roberts, S., 1997. Evolution of a metamorphic fluid and its role in lode gold mineralization in the Central Iberian Zone. Mineralium Deposita, 32, 459-474.
Nesbitt, B.E., 1988. The gold deposit continuum: A genetic model for lode mineralization in the continental crust. Geology, 15, 1044-1048.
Nesbitt, B.E., 1991. Phanerozoic gold deposits in tectonically active continental margins. In: Foster, R.P. (ed.), Gold metallogeny and exploration. Glasgow, U.K., Blackie and Sons, p.104-132.
Nesbitt, and Muehlenbachs, K., 1991. Stable isotopic constraints on the nature of the syntectonic fluid regime of the Cnadian Cordillera. Geophysical Research letters, 18, 963-966.
Oliveira, D.P.S., Quental, L.M.A.R. and Martins, L.M.P., 1997. The Portuguese sector of the Abrantes-Cordova shear Zone: Notes on the gold potential of the São Martinho area east of Alter do Chão, northern Alentejo, Portugal. In: Papunen, H. (ed.), Mineral Deposits: Research and Exploration, Where do They Meet? Proceedings of the fourth biennial SGA meeting, Turku/Finland/August 1997, 261-264.
Oliveira, J.T., Oliveira, V. and Piçarra, J.M., 1991. Traços gerais da evolução tectono-estratigráfica da Zona de Ossa Morena. Comum. Serv. Geol. Portugal, t. 77, 3-26.
Oliveira, J.T., Pereira, E., Ramalho, M., Antunes, M.T. and Monteiro, J.H., 1992. Carta Geológica de Portugal 1:500000. Serviços Geológicos de Portugal.
Ordoñes-Casado, B. O., 1998. Geochronological studies of the Pre-Mesozoic basement of the Iberian Massif: The Ossa Morena Zone and the allochthonous complexes within the Central Iberian Zone. PhD thesis, Swiss Federal Institute of Technology Zürich, ETH Nº 12.940, 233p.
Palin, J.M. and Xu, Y., 2000. Gilt by association? Origins of pyritic gold ores in the Victory mesothermal gold deposit, Western Australia. Economic Geology, 95, 1627-1634.
Pereira, M.F.C. de C., 1995. Estudo tectónico da megaestrutura de Crato-Arronches-Campo Maior: A Faixa Blastomilinítica e limite setentrional da Zona de Ossa Morena com o autóctone Centro Ibérico (Nordest Alentejano). MSc thesis, unpublished, Faculty of Science; University of Lisbon, 108p.
Pereira, M.F.C. de C., 1999. Caracterização da estrutura dos domínios setentrionais da Zona de Ossa Morena e seu limite com a Zona Centro ibérica, no nordeste alentejano. Ph.D. thesis (unpubl.), University of Évora, 114p.
Pereira, M. F. and Silva, J.B., 2001. A new model for the Hercynian Orogen of Gondwanan France and Iberia: discussion. Journal of Structural Geology, 23, 835-838.
Pereira, M.F. and Silva, J.B., 2002. Discussion on “U-Pb geochronology for the Barreiros tectonised granitoids and Arronches migmatitic gneisses: Tomar Cordoba Shear Zone, east central Portugal” by D.P.S. De Oliveira, M. Poujol and L.J. Robb, Rev. Soc. Geol. España 15 (3-4), 247-252.

Phillips, G.N. and Groves, D.I., 1983. The nature of Archean gold-bearing fluids as deduced from gold deposits of western Australia. Journal of the Geological Society of Australia, 30, 25-39.

Phillips, G.N. and Powell, R., 1993. Link between gold provinces. Economic Geology, 88, 1084-1098.

Pinto, M.S., Casquet, C., Ibarrola, E., Corretgé, L.G. and Ferreira, M.P., 1987. Sintese geocronologica dos granitóides do maciço Hespérico. In: Bea, F., Carnicero, A., Gonzalo, J.C., Plaza, M. L., Alonso, M.D.R. (eds.), Geologia de los granitoides y rocas asociadas del macizo hesperico. Libro de Homenaje a L.C. Garcia de Figuerola, p69-86.

Powell, R., Will, T.M., and Phillips, G.N., 1991. Metamorphism in Archaean greenstone belts: calculated fluid compositions and implications for gold mineralization. Journal of Metamorphic Geology, 9, 141-150.

Quesada, C. and Munhá, J., 1990. Metamorphism. In: Pre-Mesozoic Geology of Iberia, RD Dallmeyer and E. Martinez Garcia, (eds.), Springer Verlag Berlin Heidelberg, 314-319.

Quesada, C. and Dallmeyer, R.D., 1994. Tectonothermal evolution of the Badajoz-Cordòba Shear Zone (SW Iberia): characteristics and $^{40}Ar/^{39}Ar$ mineral age constraints. Tectonophysics, 231, 195-213.

Qiu, Y. and McNaughton, N.J., 1999. Source of Pb in orogenic lode gold mineralization: Pb isotopic constraints from deep crustal rocks from the southwestern Archaean Yilgarn craton, Australia. Mineralium Deposita, 34, 366-381.

Ramsay, W.R.H., Bierlein, F.P., Arne, D.C. and van den Berg, A.H.M., 1998. Turbidite-hosted gold deposits of Central Victoria, Australia; their regional setting, mineralization styles, and some genetic constraints. Ore Geology reviews, 13, 131-151.

Ribeiro, A., Antunes, M.T., Ferreira, M.P., Rocha, R.B., Soares, A.F., Zbyszewski, G., Almeida, F.M. de, Carvalho, D. de and Monteiro, J.H., 1979. Intoduction à la géologie générale du Portugal, Serviços Geológicos de Portugal, 114p.

Ridley, J.R., Dalstra, H.J. and Bloem, E.J.M., 1997. Metamorphic and structural evolution of amphibolite-facies and lower grade terrains of the Yilgarn craton. In: Cassidy, K.F., Whitaker, A.J. and Liu, S.F. (eds.), An International Conference on Crustal evolution, Metallogeny and Exploration of the Yilgarn Craton-An Update. Australian Geological Survey Organisation, Record 1997/41, 77-82.

Ridley, J.R. and Diamond, L:W., 2000.Fluid chemistry of Orogenic Lode Gold Deposits and implications for genetic models. SEG Reviews, 13, 141-162.

Roberts, S., Sanderson, D.J., Dee, S. and Gumiel, P., 1991. Tectonic setting and fluid evolution of auriferous quartz veins from the La Codosera area, western Spain. Economic Geology, 86, 1012-1022.

Rock, N.M.S., Groves, D.I., Perring, C.S. and Golding, S.D., 1989. Gold lamprophyres, and porphyries: what does their association mean? In: Keays, R.R., Ramsay, W.R.H. and Groves, D.I. (eds.), The Geology of Ore Deposits: The perspective in 1988, Economic Geology Monograph 6, 609-625.

Ryan, R.J. and Smith, P.K., 1998. Gold mineralization in Nova Scotia. Ore Geology reviews, 13, 153-183.

Sangster, A.L., 1992. light stable isotope evidence for a metamorphogenic origin for bedding-parallel gold veins in Cambrian flysch, Meguma Group, Nova Scotia. Exploration and Mining Geology, 1, 69-79.

Schäfer, H.J., Gebauer, D., Nagler, T.F. and Eguiluz, L., 1993. Conventional and ion-microprobe U-Pb dating of detrital zircons of the Tentudía Group (Série Negra, SW Spain): implications for zircon systematics, stratigraphy, tectonics and the

Precambrian/Cambrian boundary. Contributions to Mineralogy and Petrology, 113, 289-299.
Schidlowski, M., 1988. A 3.800-million-year isotopic record of life from carbon in sedimentary rocks. Nature, 333, 313-318.
Shelley, D. and Bossière, G., 2000. A new model for the Hercynian Orogen of Gondwanan France and Iberia. Journal of Structural Geology, 22, 757-776.
So, C.-S. and Yun, S.-T., 1997. Jurassic mesothermal gold mineralization of the Samhwanghak Mine, Youngdong area, Republic of Korea: Constraints on hydrothermal fluid geochemistry. Economic Geology, 92, 60-80.
Solá, A.R., 1996-1999. Relatório de Estágio: Processos petrogenéticos de Maciços Graníticos. Petroquímica do Complexo Eruptivo de Nisa. IGM Internal Report, 33p.
Turner, F.J., 1981. Metamorphic Petrology: Mineralogical, Field and Tectonic Aspects (2nd. Ed.). Hemisphere Publishing Corporation, 524p.
Winkler, H.G.F., 1979. Petrogenesis of Metamorphic Rocks. Springer Verlag New York, Heidelberg, Berlin, 348p.

_____oOo_____